CRCLEME
Cooperative Research Centre for
Landscape Environments
and Mineral Exploration

MINERAL RESOURCES NEW SOUTH WALES

OPEN FILE REPORT SERIES

REGOLITH, GEOMORPHOLOGY, GEOCHEMISTRY AND MINERALISATION OF THE SUSSEX-COOLABAH AREA IN THE COBAR-GIRILAMBONE REGION, NORTH-WESTERN LACHLAN FOLDBELT, NSW

A joint project between CRC LEME and NSW DMR

R.A. Chan, R.S.B. Greene, N. de Souza Kovacs,
B.E.R. Maly, K.G. McQueen and K.M. Scott

CRC LEME OPEN FILE REPORT 148

March 2003

(CRC for Landscape Evolution and Mineral Exploration Report 166 /
NSW DMR Report GS2001/319, 2001.
Second impression 2003)

REGOLITH, GEOMORPHOLOGY, GEOCHEMISTRY AND MINERALISATION OF THE SUSSEX-COOLABAH AREA IN THE COBAR-GIRILAMBONE REGION, NORTH-WESTERN LACHLAN FOLDBELT, NSW

A joint project between CRC LEME and NSW DMR

R.A. Chan, R.S.B. Greene, N. de Souza Kovacs,
B.E.R. Maly, K.G. McQueen and K.M. Scott

CRC LEME OPEN FILE REPORT 148

March 2003

(CRC for Landscape Evolution and Mineral Exploration Report 166 /
NSW DMR Report GS2001/319, 2001.
Second impression 2003)

CRC LEME is an unincorporated joint venture between CSIRO-Exploration & Mining, and Land & Water, The Australian National University, Curtin University of Technology, University of Adelaide, Geoscience Australia, Primary Industries and Resources SA, NSW Department of Mineral Resources and Minerals Council of Australia.

Headquarters: CRC LEME c/o CSIRO Exploration and Mining, PO Box 1130, Bentley WA 6102, Australia

The Girilambone (Cobar-Bourke) Project is providing a new knowledge base and developing methodologies for improved mineral exploration in areas of regolith cover in central western NSW. This integrated project has a multidisciplinary team with skills in regolith geology, geomorphology, bedrock geology, geochemistry, geophysics and soil science, working to understand the processes and controls on element dispersion in a variable regolith terrain. This report forms part of a planned series of three reports on work in progress.

Copies of this publication can be obtained from:
The Publications Officer, c/- CRC LEME, CSIRO Exploration and Mining, PO Box 1130, Bentley, WA 6102, Australia. Information on other publications in this series may be obtained from the above, or from http://crcleme.org.au/
Cataloguing-in-publication:
Chan, Roslyn A. et al
Regolith, geomorphology, geochemistry and mineralisation of the Sussex-Coolabah area in the Cobar-Girilambone region, North-Western Lachlan foldbelt, NSW
ISBN 0 643 06842 2
1. Regolith – New South Wales
2. Geochemistry – New South Wales
3. Landforms – New South Wales
I. Chan, R.A.
II. Title
CRC LEME Open File Report 148.
ISSN 1329-4768

Addresses and affiliations of authors

R.A. Chan, N.de Souza Kovacs, B.E.R. Maly
CRC LEME
C/- AGSO Geoscience Australia
Minerals Division
GPO Box 378
Canberra ACT 2601
Australia

R.S.B. Greene
CRC LEME
C/- Australian National University
School of Resources, Environment and Society
PO Box 4
ACT 0200

K.G. McQueen
CRC LEME
C/- University of Canberra
Faculty of Applied Science
Division of Science and Design
ACT 2601

K.M. Scott
CRC LEME
C/- CSIRO
Division of Exploration and Mining
PO Box 136
North Ryde
NSW 1670

Abstract

A joint study by NSW Department of Mineral Resources (DMR) and the Cooperative Research Centre for Landscape Evolution and Mineral Exploration (CRC LEME) of the Sussex-Coolabah area was undertaken to assist geological mapping and mineral exploration in the relatively unknown Girilambone belt of the Lachlan Fold Belt. This study was based around a shallow drilling program of 138 air core drill holes, spaced mostly at 1 km intervals along 3 road traverses. This CRC LEME report details the regional mineralisation, weathering and geochemical setting, based on previous studies, and the methodologies and results of investigations of the regolith geology within the study area. This report complements the NSW DMR report (GS2001/200).

Regolith landform mapping, incorporating remotely sensed data, and selected soil analyses enabled identification of the distribution and landform association of dominant surficial regolith materials in the study area, and their processes of formation. Much of the surficial material is sheetwash colluvium with intervening modern alluvial tracts, and minor residual soils: an aeolian component appears to be widespread in the top 0.5 to 3 m of soils. Enhanced airborne magnetics enabled identification of subsurface magnetic sediments associated with widespread networks of palaeovalleys. Field and microscopic logging of the drill holes, assisted by Portable Infrared Mineral Analyser (PIMA) analysis, enabled differentiation of transported and *in situ* regolith and the description of material attributes. PIMA analysis also identified variations in mineralogy of the highly weathered sedimentary bedrocks. Regolith profiles were interpreted for all drill holes, and used as the basis for deriving sections along the 3 traverses. The areal data from the regolith landform mapping and the magnetics provide a context for extrapolation from the sections, and thereby an indication of the 3D regolith architecture of the study area. Palaeosediments cover about 50% of the area. They infill palaeovalleys up to 40 m in depth and 7 km wide, and overtop palaeohighs in places.

Regolith and bedrock samples were geochemically analysed for a suite of 22 elements. A number of *in situ* and displaced geochemical anomalies worthy of follow up investigation were detected. Ten profiles with anomalous or interesting geochemistry (involving 7 elements) are discussed with regard to the relationship between geochemistry, mineralogy and regolith setting. Mafic dykes (commonly with high Cr) are indicated by combined X-ray Diffraction and PIMA analyses of saprolite.

The regolith and landform evolution of the Sussex-Coolabah area is placed in a regional framework and is taken back to the Mesozoic, allowing geochemical anomalies to be placed in an evolutionary context.

CONTENTS

1 INTRODUCTION

Cobar is located in western New South Wales, approximately 550 km north west of Sydney. The project area is centred on the Cobar 1:250,000 topographic map sheet, covering mainly the 1:100,000 topographic map sheets of Sussex and Coolabah (Figure 1).

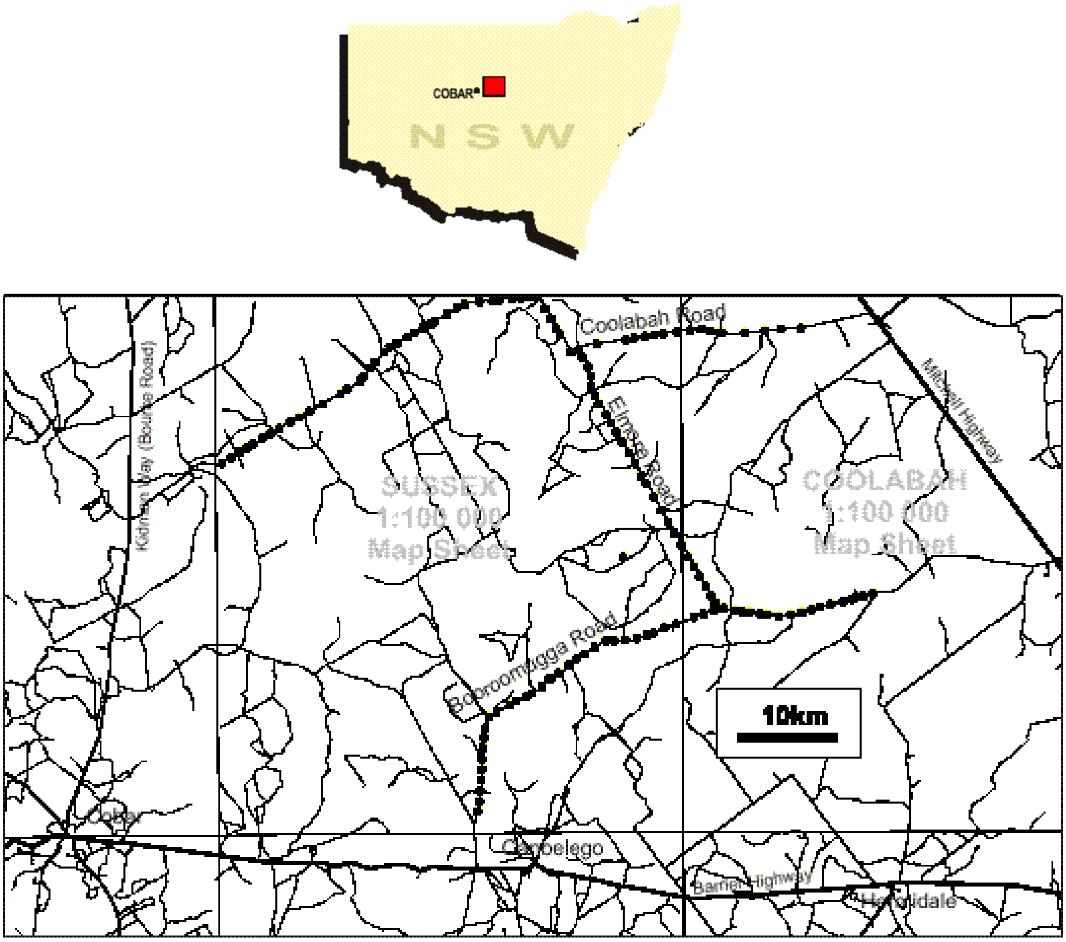

Figure 1 Location of Study Area.

Cobar has a semi-arid climate with a mean maximum summer temperature of 34.6°C (January) and a mean winter maximum temperature of 15.5°C (July). The mean minimum temperature is 19.7°C (January) and 4.3°C (July) for summer and winter respectively. Cobar has an average annual rainfall in excess of 300mm and the wind is generally from the N – NW (9 am) changing to S – SW in the afternoon (3 PM) (Bureau of Meteorology, 2001).

The aim of this study is to assist the geological mapping and exploration of the Girilambone belt by providing a more detailed understanding of the regolith geology of the Sussex-Coolabah area. The study was conducted in collaboration with the Geological Survey of NSW (NSWDMR). The approach taken was to log and geochemically analyse 138 shallow air core drill holes at approximately 1 km spacing to provide detailed data to study, and to interpret in the wider regolith and geomorphic context based on previous studies. Regolith landform mapping and analysis of surficial materials and their associated present geomorphic processes, along with inspection of processed magnetic data to map subsurface regolith materials, help place the drilling data in context. Derived regolith profile sections manifestly indicate the evolution of regolith and landforms through time, which can help to explain certain geochemical anomalies. Regolith attributes may assist in determining bedrock lithology and distinguishing weathering and alteration processes.

Different aspects of this study have been investigated and reported on by the various authors. R.A. Chan led the management and scientific integration of this CRC LEME study, as well as interpreting the regolith profile sections, the palaeodrainage, and the regolith and landform history of the area. R.S.B. Greene contributed the analysis and interpretation of possible aeolian dust in a few surface soil samples. N. de Souza Kovacs carried out PIMA analysis on selected drill hole materials, and entered microscopy attribute data into AGSO's Deviant database. B.E.R. Maly processed remotely sensed data, produced the regolith map over the eastern half of the study area, and carried out both field and microscope logging of drill hole materials. K.G. McQueen provided the context setting for weathering and geochemical dispersion based on a synthesis of previous studies, and an overview of regional mineralisation. K.M. Scott interpreted geochemical anomalies and integrated mineralogy results.

2 REGIONAL SETTING

2.1 Geomorphic Outline

The study area sits mainly within the upper catchment of northerly flowing tributaries of the Darling River. The eastern edge of the study area is within the catchment of the northeast flowing headwaters of the Macquarie and Bogan Rivers. The village of Coolabah sits on top of this drainage divide. To the southwest of the study area drainage flows west into the Murray Basin sand plains, and further south of the study area are the south draining headwaters of the Lachlan River catchment (Figure 2). The topographic profiles from the Lachlan River in the south to the Darling River in the north (Figure 3) reflect this upper headwater location of relatively high local elevation (mostly 200-300 m above sea level) and up to 50 m relief. The average gradient of the profiles is longer and gentler to the Darling and Bogan Rivers in the north than to the Lachlan River to the south. Figure 2 summarises the dominant landforms and associated depositional regolith for the Cobar region from 1:500 000 regolith landform mapping (Gibson, 1999). The study area was mapped as dominantly erosional plains (less than 9 m relief) and rises (less than 30 m relief) with the headwaters of a north flowing alluvial valley.

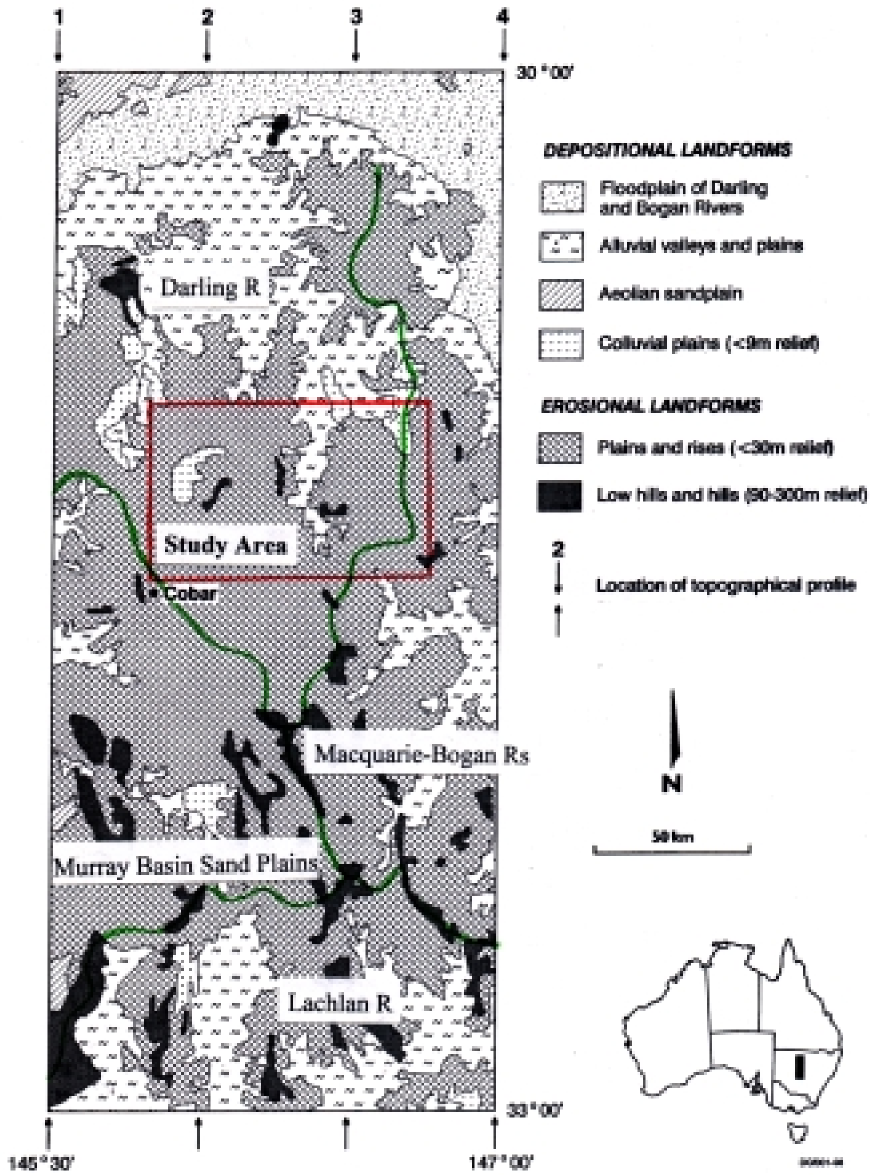

Figure 2. Location of study area in relation to major drainage catchments and their divides, and regional landforms and associated depositional regolith (after Gibson, 1999)

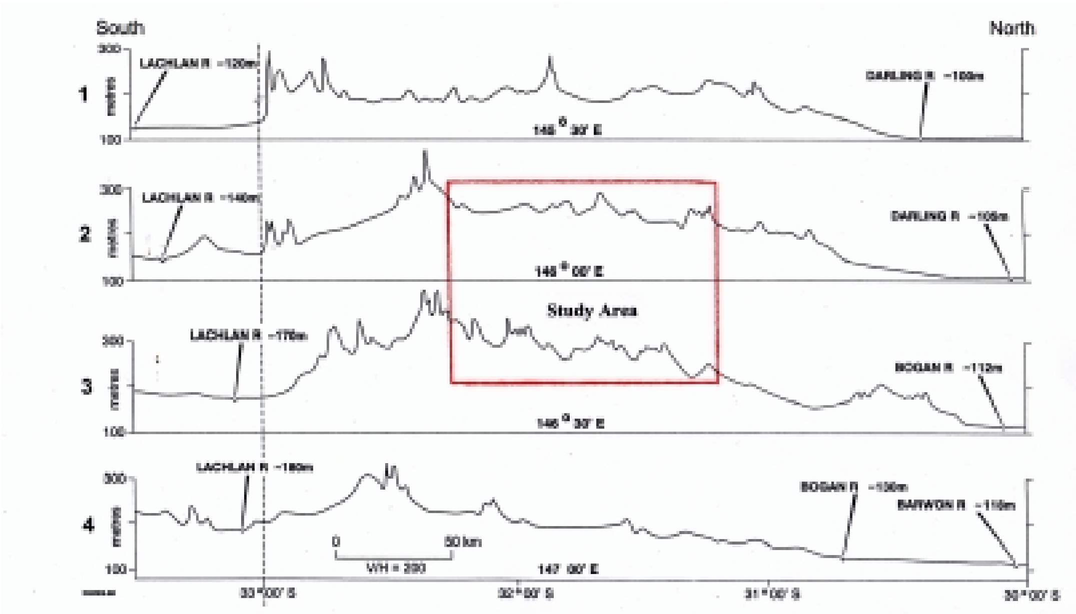

Figure 3. Location of study area on topographic profiles from the Lachlan River in the south to the Darling River in the north (after Gibson, 1999).

2.2 Previous Regolith Studies

Previous regolith studies in the Cobar area cover regional mapping at 1:500,000 scale (Gibson, 1999), 1:250,000 and 1:100,000 scales (Spry, in prep.) and more detailed mapping at 1:25,000 (Gonzalez, 2001). The Cobar-Girilambone project area can be located, in part, on all of these map sheets.

Apart from regolith mapping, specific regolith features have been studied in detail in the Cobar area. On a regional scale, there have been investigations into the type and distribution of soils in the Cobar region (Jessup, 1961) and the contribution of parna to regional soils (Greene and Tongway, 1989, Greene, 1992). Jessup studied the evolution of the two youngest soil layers in the southeastern portion of the Australian arid zone, the Parakylia and Bookaloo Layers. The purpose of the investigations were to discuss the two layers and the origin of the parent materials over two extensive and representative areas in the south-eastern portion of Australia's arid zone, including central South Australia and North-Western New South Wales-South-Western Queensland.

An important geochemical sampling medium and one that is directly relevant to the Cobar region is lag. Alipour *et al*, (1997) investigated the characteristics of magnetic and non-magnetic lag in the Cobar area. This study involved collecting lag along a number of traverses across two field sites. The magnetic and non-magnetic fractions were separated, pulverised and geochemically analysed. Results showed Cu concentrations tended to peak in the ferrolithic lag component, and Zn followed a similar trend to Cu, with Pb, Cr and Fe generally highest in the magnetic component. This has important implications for the present study area, as a large proportion of the study area is covered by palaeovalley sediments and contain large quantities of magnetic and non-magnetic materials, though much is buried by modern surface sediments.

On a more detailed level Cairns *et al.*, (2001) investigated the mineralogical controls on element dispersion in regolith near The Peak, Cobar. The results showed the importance of secondary Fe and Mn oxides and oxyhydroxides as major hosts for base metal cations within *in situ* regolith developed in a dominantly erosional setting. Cairns *et al.,* (2001) identified manganese minerals as importanthosts for Pb and Zn, and suggest that the goethite-rich component of the regolith, including overlying lags, is the most appropriate sampling medium for base metal exploration.

In comparison to this present study, Ford (1996) used drainage channel morphology to re-interpret the northeastern margin of the Cobar Basin and examined its implication for mineral exploration. The study looked at drill samples collected from Rotary Air Blast (RAB) drilling of an extensive palaeovalley system between 5 km and 25 km north of Cobar, in which Ford was attempting to identify an optimum method for exploring beneath fluvial deposits in the area. Ford concluded that the position of the Rookery Fault follows the trend of the palaeovalley, thus suggesting that the previously interpreted position of the Rookery Fault is approximately 2km east of Ford's proposed position.

2.3 Economic Geology and Known Styles of Mineralisation

The Cobar-Girilambone-Nymagee region is one of the richest mineral provinces in New South Wales. The area covered in this study lies within this region, but no significant mineralisation has yet been found. Major deposits occur in the Cobar Basin, just to the west, around Girilambone to the east, and at Canbelego and Nymagee to the south. Deposits at these sites are briefly reviewed, followed by descriptions of minor occurrences and comments on potential styles of mineralisation in the Sussex-Coolabah study area.

2.3.1 Deposits in the Girilambone Terrain

(Hosted by Cambrian-Ordovician metasedimentary and metavolcanic rocks, and some probable Late Silurian-Early Devonian sedimentary units)

The rocks and geological environments preserved in this terrain are poorly known. The sequences have been strongly deformed with probable juxtapositioning of different crustal blocks and sequences (Glen and Fleming, 2000). Known rock types include quartzose and quartzo-feldspathic sandstones, siltstones, cherts, together with minor intercalated mafic volcanics, minor conglomerates, marls and serpentinite (Suppel and Gilligan, 1993). Low grade regional metamorphism has also produced psammitic, pelitic and mafic schists. These rocks have been ascribed an Ordovician age although it is likely that some unmetamorphosed quartzites, siltstones and conglomerates belong to younger packages. Significant deposits occur in this terrain at Girilambone, Tritton and Canbelego-Mt Boppy.

2.3.1.1 Metasediment-hosted Copper Mineralisation

2.3.1.1.1 Girilambone

The Girilambone copper deposit (total resource ca 124,000 t Cu) occurs 4 km W of Girilambone and is hosted by chlorite-sericite schists and a banded quartzite member of the Caro Schist Formation, the basal formation of the Girilambone Beds (Shields, 1996). Mineralisation includes: massive sulfide lenses (up to 10 m thick) in quartzites; strongly folded, layered and banded sulfides in quartzites; and disseminated sulfides within chloritic schists. The dominant primary sulfides are pyrite and chalcopyrite, with secondary chalcocite developed in partly oxidised ores (Hellman, 1991). Malachite, azurite, cuprite and native copper occur in the main oxidised zone of the deposit, and rare phosphate minerals, including libethinite have been reported from the upper section of the oxide zone (Shields, 1996). The mineralisation appears to have been extensively modified by structural/metamorphic events, including hydrous remobilisation. Weathering has created a typical supergene profile with a 20-30 m leached zone, a carbonate-oxide zone (mainly malachite-azurite) and an enriched chalcocite "blanket" below the current water table (80-100 m below surface). It has been suggested that the dominant quartzite host rock was originally an exhalative, chemical sediment. The layered style of sulfide mineralisation within this unit has been used to suggest the deposit represents a deformed, stratiform massive volcanogenic sulfide deposit, of possibly "Besshi" type (Shields, 1996). Alternate ore genesis models suggest that the Girilambone deposits are structurally controlled, epigenetic vein and lode systems.

2.3.1.1.2 Tritton

The Tritton copper, minor gold-silver deposit (25 km SW of Girilambone) is hosted by a sequence of pelitic schists, mafic schists, greywackes and quartzites, considered part of the Girilambone Group. The mineralisation appears to be structurally controlled, consisting of lenses, pods and stringers of massive chalcopyrite-pyrite with lesser bornite and minor tetrahedrite, digenite and chalcocite (Fogarty and Hastings, 2001). The total resource is estimated at about 11 million tonnes of 2.87% copper at a 1% cutoff (Nord Pacific Ltd, 1998). Mineralisation does not outcrop. Oxidation in the area extends to a depth of approximately 60 m and supergene enrichment processes have been important at nearby outcropping deposits.

2.3.1.2 Quartz Vein and Stockwork Gold Mineralisation

2.3.1.2.1 Canbelego-Mount Boppy

Significant quartz-vein stockwork style gold mineralisation occurs near Canbelego, just south of the Sussex area. Gilligan and Byrnes (1995) suggest that there is a major lithostratigraphic control on the distribution of the mineralisation with the bulk of the mineralisation restricted to the basal sections of the Early Devonian Baledmund Formation (Kopyje Group). The major Mt Boppy deposit (14.2 t of produced gold) is hosted by conglomerates (Baledmund Formation) near an unconformity with Girilambone basement and within a tight south plunging syncline (Gilligan and Byrnes, 1995). Mineralisation consists of gold in stockwork quartz veins and zones of silicification. Breccias are also strongly developed. Minor sphalerite and galena (locally massive) are recorded from deeper levels of the Mt Boppy mine (Gilligan, 1974). The stratigraphic position of the deposit together with its form and mineralogy led Gilligan (1982) to interpret the deposit as a deformed volcanogenic exhalative deposit associated with local volcanism. Most features are also consistent with a structurally controlled epigenetic origin. Oxidation at the deposit extends to a depth of 91 m and leaching and supergene enrichment are reported to be important. Secondary minerals in the weathering zone include limonite, pyrolusite, haematite, cerussite, anglesite, gold and chalcocite (Gilligan and Byrnes, 1995).

2.3.2 Deposits in the Cobar Basin and Related Terrain

(Hosted by Late-Silurian-Early Devonian turbidites)

2.3.2.1 Cobar-type Deposits

Structurally controlled polymetallic sulfide mineralisation is a feature of the high-strain eastern margin of the Cobar Basin. Total metal production from these deposits (to 1995) includes 603,703 t of copper 639,029 t of lead, 1,185,822 t of zinc, 1,535 t of silver and 56 t of gold (Stegman and Stegman, 1996). Known mineralisation is localised along major shear and thrust-fault systems, particularly in zones of juxtaposed contrasting lithologies. Deposits are multiple vein and massive sulfide pods and lenses that are typically confined to steeply plunging pipe-like concentrations within the steeply dipping host structures. Consequently most orebodies have a small ellipsoidal surface expression and a large down plunge extension (up to >1000 m, Stegman and Pocock, 1996). Individual deposits show different metal abundances which suggest a regional scale metal zoning with copper-rich mineralisation in the south (Queen Bee deposit), copper-gold dominant (±lead-zinc-silver) mineralisation in the Cobar area, copper-zinc to the north of Cobar (CSA deposit) and lead-zinc-silver in the northwest (Elura deposit). Mineralisation is typically accompanied by siliceous and chloritic alteration and in some cases carbonate alteration (eg. Elura). Most deposits show extensive oxidised zones (to 60-100 m below surface) with variable supergene enrichment at the water table. Cobar-type deposits are considered to be of metahydrothermal origin (eg. Glen, 1987) probably requiring basin-scale fluid systems and major structures to focus fluids. Predominance of different stages of mineralisation in a multi-stage paragenetic sequence is considered to be the cause of the different metal endowments at different deposits in the Cobar field (Stegman, 2000).

At Nymagee (78 km SE of Cobar) similar polymetallic sulfide mineralisation is developed in equivalent turbidites. This deposit contains three main zones of mineralisation, which are near conformable with bedding in the enclosing sediments. The ore is dominated by pyrrhotite-chalcopyrite with some sphalerite, galena, magnetite, arsenopyrite, cubanite, tetrahedrite, bismuth and argentite. The deposit has a leached oxidised zone (to 15 m) and an underlying supergene enriched zone from which much of the copper was produced. Historic (prior to 1907) production at Nymagee was 24,800 t of copper from 428,986 t ore. Estimated remaining reserves are 435,160 t of greater than 2% Cu and 3% Pb, 7% Zn (Paterson, 1974).

2.3.2.2 Disseminated, Stockwork and Vein-type Gold Deposits

2.3.2.2.1 McKinnons

The McKinnons gold deposit (production 4.2 t Au) is a structurally controlled, epigenetic, stockwork vein system hosted in carbonate-bearing turbidites of the Early Devonian Lower Amphitheatre Group. The deposit is located close to the western margin of the Cobar Basin along the northwesterly trending Nullawarra anticline. Mineralisation consists of chalcedonic, gold-bearing quartz veins within blocks or pods of silicified host rock containing disseminated and veinlet pyrite and lower grade gold. Drilling indicates the presence of underlying base metal veins (including pyrite, galena and sphalerite), possibly related to an earlier stage of the mineralising process. The deposit has been interpreted as a shallow level "epithermal" type system related to an underlying granitic heat source (Rugless et al., 2000; Forster and Seccombe, 2000). Weathering and oxidation extend to a depth of 60-80 m and have been beneficial in releasing gold from pyrite. There is also evidence of supergene enrichment of gold (Marshall and Scott, 1999). The geochemical association at McKinnons includes Au, Ag, As, Ba, Bi, Cu, Hg, Ni, Pb, Sb, W and Zn. Primary ore minerals include pyrite, arsenopyrite, gold-electrum, galena, sphalerite, chalcopyrite and tennantite-tetrahedrite. Secondary minerals recorded from the weathering zone include goethite, haematite, supergene pyrite, gold, silver, plumbogummite, iodyrite, native mercury, amalgam, hindsalite, chlorargyrite and chalcocite. Barite has also been detected.

2.3.2.2.2 Mount Drysdale

The Mount Drysdale gold deposit (recorded production 0.81 t Au) is hosted in slates, sandstones and conglomerates (Mount Drysdale Conglomerate Member) of the Early Devonian Chesney Formation, in an area of thrust faulting with Girilambone Group rocks. The deposit is developed in a steeply dipping silicified shear zone at the eastern margin of the Cobar Basin. Mineralisation consists of an outer envelope of disseminated pyrite and pyrrhotite surrounding a zone of silicification containing three zones of richer ore. Other sulfides reported include chalcopyrite, galena and sphalerite (Gilligan and Byrnes, 1995). Significant silver has been reported at the deposit and nearby similar deposits, probably from the oxidised zone. Iron oxides, gold, silver, cerargyrite, pyrargyrite, embolite, iodyrite and iodobromite are recorded from the weathering zone (Gilligan and Byrnes, 1995). A small amount of alluvial gold (9.33 kg) was produced from a small gully on the western side of Mt Drysdale.

2.3.2.2.3 Gilgunnia

The Gilgunnia goldfield (total recorded production 0.21 t Au) is located southwest of Nymagee and consists of two areas of mineralisation hosted by sedimentary rocks of the Upper Amphitheatre Group. Mineralisation consists of bedding and cleavage parallel veins of strongly ferruginous quartz containing gold with traces of Cu, Pb and Zn. At each area there appear to be several lines of reef. The eastern most area of mineralisation (Four Mile) is located in the hinge of a tight anticline, close to underlying rhyolitic tuff. The deposits appear to be structurally controlled epigenetic veins although an alternate suggestion is that they are related to volcanogenic-epithermal processes accompanying felsic volcanism (Suppel and Gilligan, 1993). Most production at the two sites has probably come from the oxidised zones as all working are less than 80 m deep. Pyrite and minor galena are the only primary minerals recorded.

2.3.3 Mineral Deposits in the Study Area

Minor mineral occurrences and prospects are described from the Sussex-Coolabah area in the metallogenic notes for the Cobar 1:250,000 sheet (Gilligan and Byrnes, 1995). These include the following types.

1. Vein-type gold mineralisation, generally with associated base metals and typically hosted in shear zones with variable quartz veining. These occurrences are scattered throughout the Sussex area. Anomalous associated elements include As, Pb, Ag, Ba, Zn and in some cases Cu. Lead typically shows high concentrations in oxidised and gossanous materials (up to % levels). Primary minerals recorded include pyrite, pyrrhotite, gold, arsenopyrite, galena, sphalerite and chalcopyrite. Secondary minerals noted include goethite, haematite, "manganese oxides" pyrolusite, plumbojarosite and gold.

   Deposits (with Cobar metallogenic map reference number) include:

Unnamed on Coronga Downs (20)	
Chaproniere Shaft (22)	
Hidden Treasure (24)	up to 3.6 g/t Au associated with Pb, As, Ag, Ba and trace Zn.
Penningtons Tank (25)	rock samples strongly anomalous in Pb with Zn, Cu and Ag.
Mulga Prospect (26)	up to 10 g/t Au.
Cobra Shaft (77)	up to 1.95 g/t Au with anomalous As and Pb.
Everingham/Richards (78)	up to 2-6 g/t Au with anomalous As, Ba, Zn and Pb.
North Pole (80)	gossan samples show highly anomalous Cu, Pb, Zn and Ag.
The Four MS (83)	up to 10 g/t Au in breccia lode with highly anomalous Pb, Zn and Ba, minor Cu.

2. Granite-related, greisen-hosted base metal mineralisation (Cu, Pb, Zn) with minor Ag, Mo and Sn. This mineralisation is in the northwestern part of the Sussex area adjacent to an unfoliated Silurian granite (possibly I-type):

Beanbah Prospect (21)	primary cassiterite and pyrite recorded, large magnetic anomaly suggests subsurface I-type granite.

3. Vein-type copper and polymetallic deposits:

Big Reef (76)	cellular boxwork gossan shows traces of Cu, Pb, Zn and Ag also with anomalous indium reported.
Emu Tank (23)	gossan contains anomalous Cu, Zn and trace Pb.
Calcite Crystal Rise (79)	anomalous Pb, Zn and Cu associated with quartz, calcite and tourmaline.

Most of these mineral showings are poorly known and generally consist of gossanous or oxidised and leached ferruginous material outcropping at surface or exposed in shallow pits and small shafts. There has been limited modern exploration in the area (see also Fleming and Hicks, 2000).

Possibilities for more significant deposits include the following styles:

- Mt Boppy type gold mineralisation in Early Devonian metasediments (including along strike from Mt Boppy itself);
- structurally controlled vein-type, polymetallic/gold mineralisation in Ordovician low-grade metamorphic rocks, particularly related to major crustal scale structures;
- deposits associated with sub surface or poorly ouctropping granitoids;
- Girilambone-type copper mineralisation developed in Cambrian-Ordovician (?) sequences with quartzites and mafic schists after volcanic rocks;
- volcanic-hosted massive sulfide deposits associated with mafic volcanic sequences;
- platinum group element mineralisation in possible mafic-ultramafic intrusions.

Two volcanic plugs, feeders to the El Capitan leucitite lavas, have recently been detected in the area. These are developed along major structures including the northern projection of the Gilmore Fault and a possible NNW-trending splay. This indicates the possibility of other mantle-derived materials reaching the surface in this area during the Miocene.

2.4 Weathering History and Geochemical Dispersion

In the Cobar-Girilambone region there has been a complex history of weathering and regolith development, which has resulted in a variety of both *in situ* and transported components of different ages and conditions of formation. Recent dating has confirmed that many preserved weathering profiles are old and in some cases, very old.

The general landform consists of a slightly raised and modified palaeosurface of undulating, rounded ridges (up to 10 m relief) and higher residuals (up to 100 m relief) of slightly to moderately weathered Palaeozoic bedrock. This is overlain by residual, colluvial and transported gravels, lithosols and red earth soils. Weathering profiles vary considerably but are commonly between 20 and 80 m thick. There are larger areas of less weathered bedrock to the east of Cobar, over Girilambone Group basement rocks. In some places, particularly along fault zones, oxidation may extend to 100 m or more. The variable depth of weathering is also controlled by palaeodrainage networks. Throughout the area there is evidence of subtle inversion of relief and infilling of a once more deeply incised landscape. There are preserved palaeovalleys at a range of levels in the landscape. More recent watercourses and alluvial valley plains transect the terrain and contain thick deposits of alluvial and colluvial sand, silt, minor gravel and clay (Fig. 4).

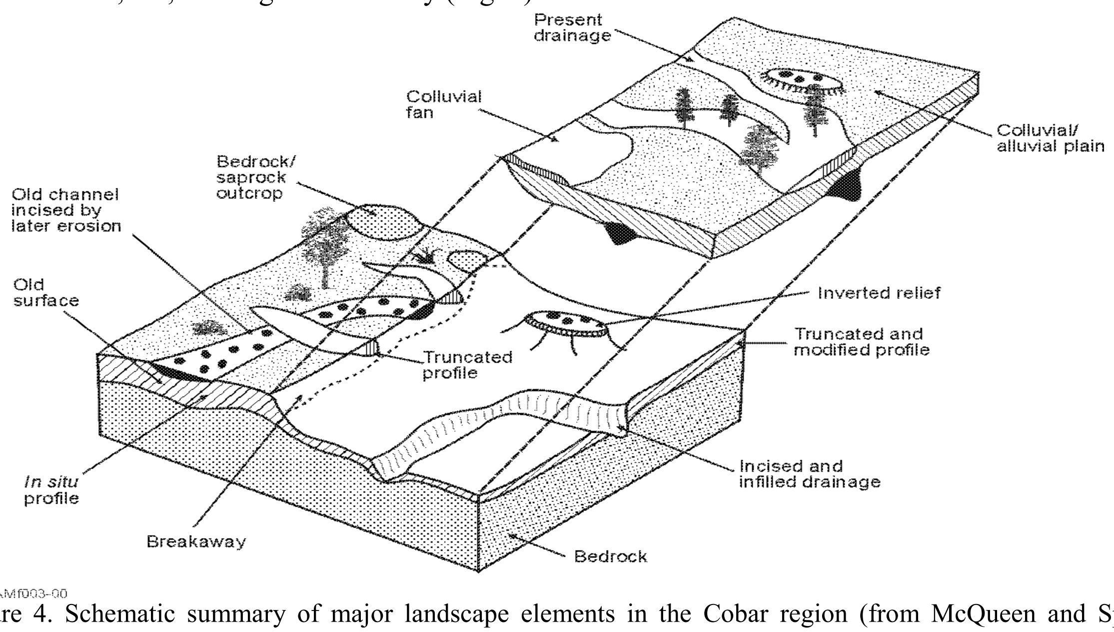

Figure 4. Schematic summary of major landscape elements in the Cobar region (from McQueen and Spry, 2000).

Areas of ferricrete, silcrete, silicified saprolite/bedrock and more recent calcrete are preserved in different parts and levels of the landscape. A variety of surface lag, including fragments of bedrock, vein-quartz, ferruginous materials from the weathering profile, calcrete and silcrete, is present over much of the land surface. This lag has undergone varying degrees of transport, depending on the particular landscape and palaeolandscape setting. The red earth soils contain a significant aeolian component and reworked aeolian deposits of silt and clay are also present in parts of the area, particularly in the modern drainage (Jessup, 1961; Tan et al., 1998). Pedogenic hardpan is developed in some of the soil profiles on the lower slopes and flats (Walker, 1991).

Weathering profiles show considerable ferruginisation, particularly near the surface, however in most cases they are not complete "lateritic" profiles and many are the products of concomitant ferruginisation and erosional stripping. Typical well preserved profiles consist of a layer of surface lag (variably ferruginous) overlying, a red silty loam soil (commonly less than 1 m thick), with an underlying highly ferruginous zone passing down into a ferruginous mottled zone (1-2 m). This in turn overlies saprolith (commonly 2-20 m thick). Most bedrock lithologies have a low iron content (<5% FeO) and significant leaching of soluble components and residual or lateral enrichment of iron by solution processes would be required to account for the highly ferruginous upper parts of many profiles (e.g. 3-10 times concentration of Fe_2O_3). Concentration of iron oxides well above present water table levels could imply significant surface lowering (including by chemical solution) as well as lowering of water table levels from their palaeo-positions. In very deep profiles concentrations of iron oxides also occur at lower levels, in association with the present water table level and possibly palaeo watertable stillstands, and around iron-rich primary zones such as pyritic mineralisation. Examples of some different weathering profiles are shown in Figure 5.

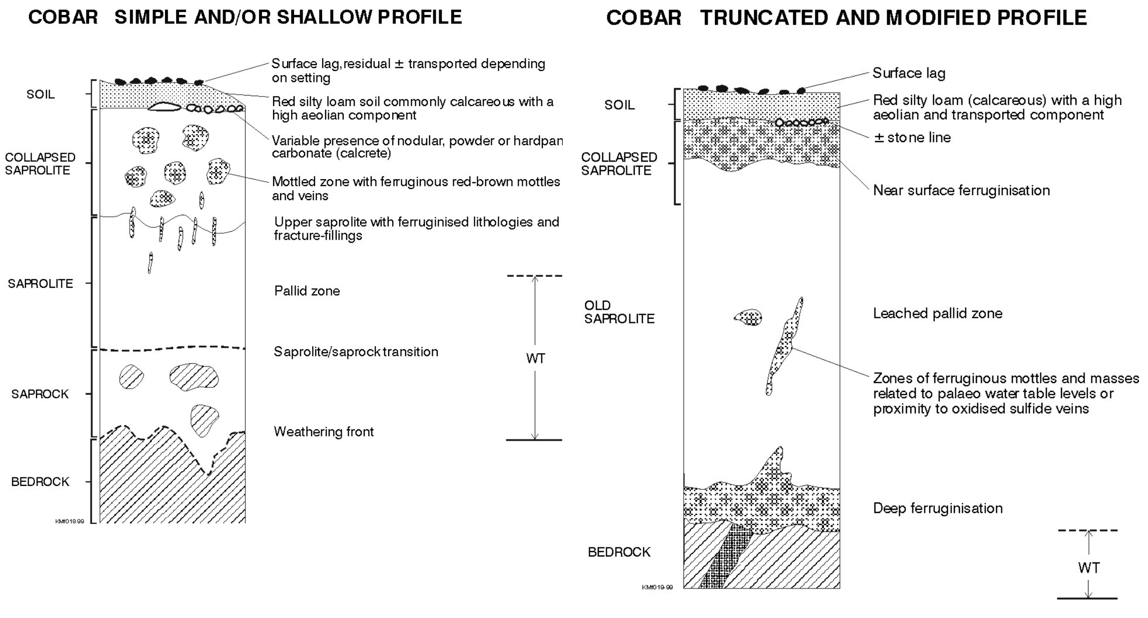

Figure 5. Examples of some different weathering profiles from the Cobar region.

2.4.1 *Weathering History*

Preliminary dating work at four sites in the Cobar area has established a framework for the weathering history of this region (B. Pillans pers. comm. 2001). The sites are at Wilga Tank (41 km NE of Cobar), Elura (41 km NW of Cobar), McKinnons (35 km SW of Cobar) and New Cobar (2.5 km S of Cobar). At Wilga Tank, a ca. 20 m deep weathering profile characterised by a ferruginous mottled zone and underlying bleached saprolite is preserved beneath a dissected basalt flow. This buried profile is similar to those common throughout the region. An adjacent volcanic plug and lava flows 8 km to the north have been radiometrically dated at 14.87 (±0.15) Ma (Phillips, 2001) and 15.2

Ma respectively (Sutherland, 1985). Weathering profiles on the basalts are thin without significant ferruginisation. Palaeomagnetic dating of the upper part of the sub-basaltic weathering profile has yielded a Middle Miocene age, similar to that of the basalts. Palaeomagnetic dating of ferruginous mottles in saprolite from a quarry just north of Elura mine has indicated two periods of iron mobilisation. These occurred in the Latest Cretaceous to Early Palaeocene (60±10 Ma) and the Middle Miocene (12±3 Ma). Oxidised saprolite from the McKinnons open pit yielded two similar ages of Latest Cretaceous to Early Palaeocene and Middle Miocene. At the New Cobar open pit, palaeomagnetic dating of oxidised saprolite (after Early Devonian shales and siltstones) has indicated a Jurassic age (ca. 180 Ma) for the ferruginisation.

The initial dating results suggest a consistent, possibly widespread, ferruginous weathering extending into the Middle Miocene and an older, Early Palaeocene ferruginisation preserved at some sites. This is consistent with the two prominent periods of weathering recognised by Idnurm and Senior (1978) in the Eromanga Basin, dated by them at 60±10 Ma and 30±15 Ma (the latter fits the Mid Miocene using current polar wander path data). Throughout the earlier Cainozoic, regional climates were episodically warm and wetter (McGowran and Li, 1998). The period just prior to the Middle Miocene (16 Ma) was characterised by hot climatic conditions, high global sea levels and a major marine incursion in the Murray Basin to the southwest. This would have inhibited erosion and promoted profile development, particularly as conditions were characterised by high perennial rainfall and high watertable levels From the Middle Miocene conditions became drier and falling watertables would have allowed oxidation and dehydration of the profiles, precipitating stable iron oxides. This is consistent with the Middle Miocene age for ferruginous materials in most of the profiles. Ferruginous deep weathering appears to have been restricted after the Middle Miocene, as suggested by the limited profiles on the basalts of this age. Quartz-rich Cretaceous sediments are preserved in topographically inverted palaeovalleys remnants in the Cobar area, possibly consistent with an earlier period of stable exposure and ferruginous profile development. The older Jurassic age preserved in the weathering profile at New Cobar suggests that this profile has either been preserved close to the surface since this time without much detectable modification or buried and re-exposed much later. It would appear that the other sites (eg. Elura and McKinnons) have only been exposed since the Latest Cretaceous or had any older profiles removed by significant erosional stripping prior to this time. It is interesting that the dispersion patterns for base metals and gold are different for the McKinnons and New Cobar settings. This reflects different chemical and ferruginisation conditions, which probably relate to the different histories of the regolith profiles and varying abundance of iron.

2.4.2 Geochemical Dispersion Processes

The long and complex weathering history of the Cobar-Girilambone region has complicated secondary geochemical dispersion processes. Predominance of warm and humid weathering conditions through the Early and Mid Tertiary, together with likely high water table levels, lead to variable leaching of base metals and residual concentration of gold over mineralised zones exposed during this period. Uptake and fixing of metals in ferruginous components of the regolith, combined with erosional stripping and widespread transport of surface lag, has resulted in extensive mechanical dispersion of geochemical anomalies.

Subsequent change to a more arid climate (largely since the Mid Miocene), continued erosional stripping and deposition of transported materials has led to the superimposition of additional chemical changes in the pre-existing regolith and its contained mineralisation. These processes have led to hydromorphic and mechanical dispersion of gold and masking of primary and secondary deposits in a complex regolith. In some parts of the region, aeolian material has also been deposited and become intimately intermixed with the soils.

Evidence for at least two episodes of ferruginisation related to intense chemical weathering, dating back to the Late Cretaceous adds to the complexity. Evidence of Jurassic exposure and weathering in at least one area, possibly followed by burial and exhumation, is a further complication.

In the Cobar area there is a range of *in situ* weathering profiles related to landscape setting and these show different styles of element dispersion. For example, in the Cobar Goldfield, profiles typically show good preservation of base metal and pathfinder element anomalies, but some depletion of gold in the upper parts, possibly due to mobilisation by chloride-rich groundwaters. Ferruginous lags in this setting commonly retain and accentuate base metal and gold anomalies. In other areas with very deep leached profiles and where water table levels have dropped and the upper parts of the profile have been stripped, gold may be retained in the strongly oxidised zone below the original water table. These perched saprolite zones can be depleted in As, Ag, Bi, Cu, Ni, Sb and Zn, particularly where they lack a ferruginous component. Thus, depending on the setting, polymetallic/gold mineralisation may show significant surface anomalies in only a limited number of elements. Lead is commonly less mobile in the weathering profiles of the Cobar region, typically becoming fixed in alunite-jarosite group minerals (e.g. plumbogummite) or Pb-Mn minerals (such as coronadite). In most environments goethite is a major host for metal ions and arsenic. Hematite and manganese oxides/oxyhydroxides are of lesser importance while alunite-jarosite group minerals, and a range of other sulfates and chlorides are additional host phases, particularly where there has been element dispersion under late-stage arid conditions. Typical mineral hosts for metals and As at strongly mineralised sites in the Cobar area are listed in Table 1. During exploration it is important to take into account the differential leaching and fixing of metals and the variations related to particular histories preserved in different weathering profiles.

Table 1. Major host phases for pathfinder elements in near surface regolith over ore deposits, Cobar area.

Iron oxides/oxyhydroxides		***Manganese oxides/oxyhydroxides***	
Goethite*	Zn, Cu, As, (Pb, Bi, Sb)	Cryptomelane group *	Pb, Ba
Hematite*	Pb, Cu, Zn, Bi, As	Lithiophorite *	Zn, Cu
Maghemite	?	Coronadite *	Pb

Sulfates		***Chlorides/Phosphate/Arsenates***	
Alunite-jarosite*	mostly Pb	Chlorargyrite *	Ag
Beudantite	Pb,Ag	Pyromorphite	Pb
Plumbogummite *	Pb	Mimetite	Pb, As
Philipsbornite *	Pb, As		
Hinsdalite *	Pb, Cu, Zn	Carbonates	
Hidalgoite	Pb, As	Malachite-azurite	Cu
Anglesite	Pb	Calcite-dolomite	Au

KM01 2-01

Concentration and fixing of metals in iron oxides/oxyhydroxides, surface concentration of these in lags, followed by recycling of ferruginous lag through the multi-stage landscape history, is a major process for element dispersion and development of widespread displaced anomalies. Locating the source of these (in some cases, large) displaced geochemical anomalies requires careful analysis of the landscape history and reconstruction of the palaeodrainage networks for different landscape stages. Soil geochemistry can be complicated by the variable presence of an aeolian component in many of the soils of the region. This extraneous material can act as a dilutant to the A and upper B horizons and its possible presence needs to be considered when designing soil sampling programs (eg. by selecting an appropriate size fraction). Work around the Cobar Goldfield (McQueen et al., 2000) has shown that there is a relationship between regolith carbonate accumulations (calcrete) and gold and that dispersed gold is detectable in this sampling medium in both *in situ* and transported regolith (Fig. 6.).

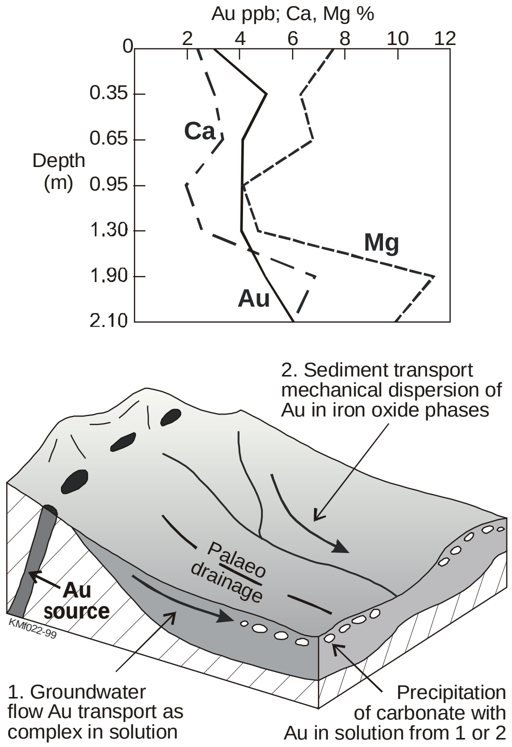

Figure 6. Schematic model showing possible pathways for lateral dispersion of Au and subsequent concentration in regolith carbonate accumulations. The geochemical profile is from near the Airport South locality, 8 km southwest of Cobar (from McQueen et al., 2000).

3 SUSSEX-COOLABAH DRILLING PROGRAM

Drilling occurred along three transects namely the Booroomugga, Elmore and Coolabah Roads. A total of 138 holes were drilled using a small 6-wheel aircore rig supplied by Geological Ore Search, Cobar. The drilling was conducted at approximately 1-3km spacing, with an average depth of 18.6m and a total depth of 2,565m achieved during the program (see also Fleming *et al.*, 2001).

3.1 Remotely Sensed Data

Initial discrimination of regolith-landform units was achieved through the use of remotely sensed data (*eg*. radiometrics, magnetics, DEM) and aerial photographs (scale of 1:82,000). The airborne digital data was supplied by NSW DMR and was acquired as part of their Discovery 2000 Initiative. Some manipulation of the remotely sensed data (*eg*. magnetics and radiometrics) was necessary to enhance the imagery's detail, including filtering and band manipulation. The software used for the manipulation and interpretation of this data included ArcView 3.1 and ERMapper 5.5. Confirmation of initial regolith-landform discrimination was gained through landform and regolith descriptions whilst in the field.

3.1.1 Magnetics

The magnetic imagery was used to determine the spatial distribution of palaeovalleys within the field area, as well as help define any changes in lithology and/or structural setting. Three derivatives of magnetic images (1VD, 1.5VD and 2VD) were compared to find out which image provided the most detailed information on the distribution of palaeovalleys within the field area. The 1.5VD magnetic image provides the most detailed information and was therefore used to mark palaeovalley boundaries and highlight the palaeovalley drainage divides.

The 1.5VD Magnetic image (see back of hardcopy report) shows approximately 40% of the Sussex-Coolabah study area covered by palaeovalleys containing magnetic sediments. Finer, less magnetic drainage systems are also present (Figure 7).

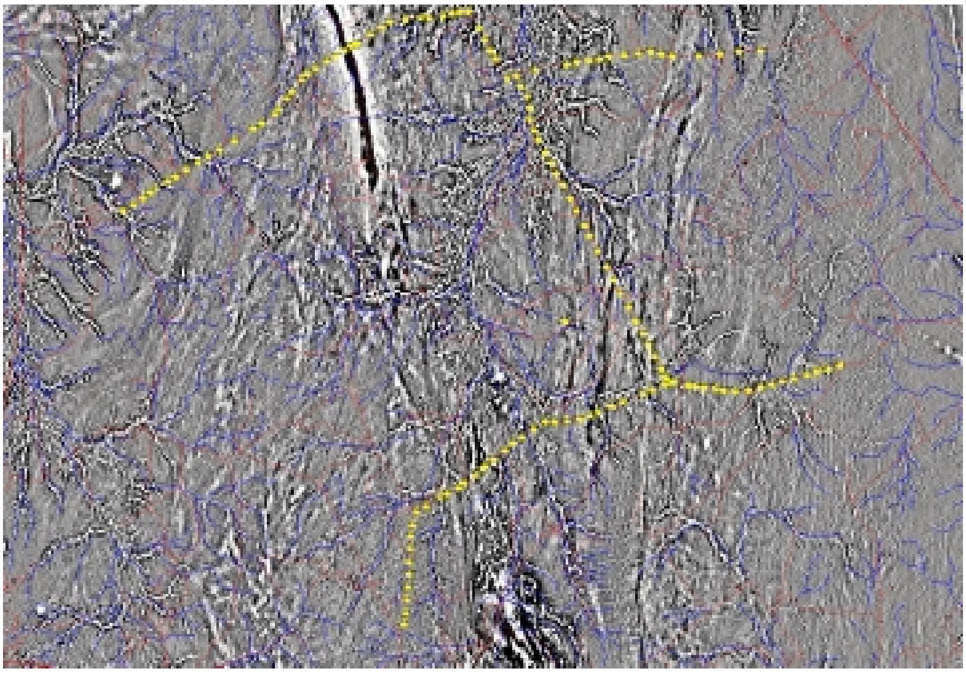

Figure 7. Airborne magnetic image of the Sussex-Coolabah area.

3.1.2 Radiometrics

Gamma spectroradiometrics (radiometrics) imagery was used to discriminate between changes in surface sediment composition within the project area. The imagery that was used included a 3 band colour composite (K, Th, U), total count and single bands of K and Th. The radiometrics composite, displayed as a Red:Green:Blue (R:G:B) image, was also used in conjunction with the 1.5VD magnetics image to investigate any correlations between the two images. This process involved overlying the magnetic image with the radiometric image in ErMapper 5.5 and then adjusting the transparency of the radiometric image so that the underlying magnetic image was also visible. Any notable features relating to the two images could then be identified.

The KThU image (displayed as a R:G:B band combination) shows prominent areas of high thorium (Green). The areas indicate the presence of magnetic gravels, which are abundant on the edges of the modern Mulga Creek drainage system (Figure 8).

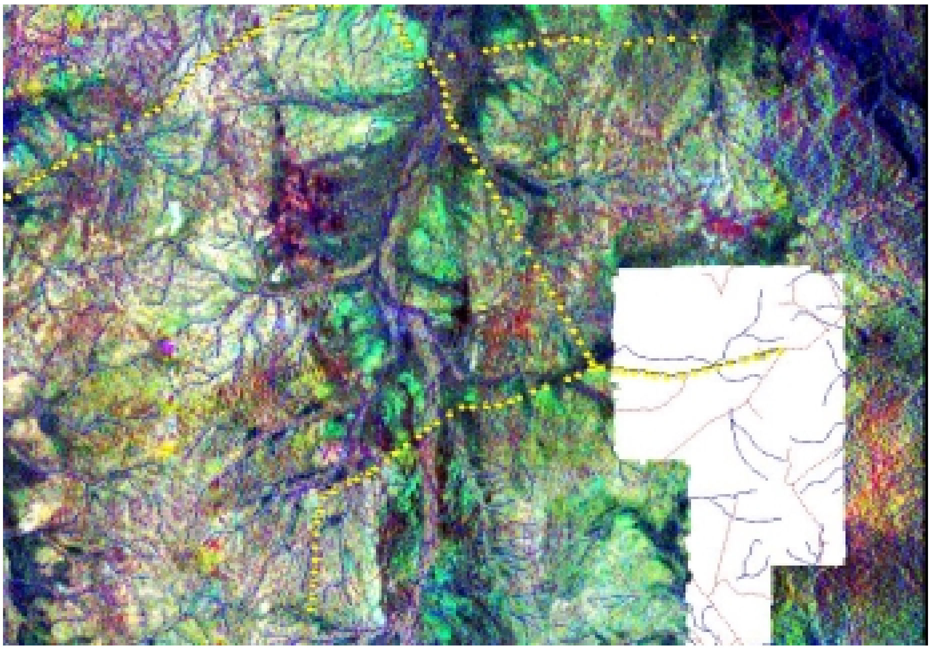

Figure 8. Three band (K,Th,U) composite radiometric image of the Sussex-Coolabah area.

3.1.3 Combined Magnetics-Radiometrics

This image is a combination of both the magnetics 1.5VD and the KThU (R:G:B) composite. This image shows that the high thorium values are restricted to palaeovalleys in certain areas that have a surface lag of maghemite. (Figure 9).

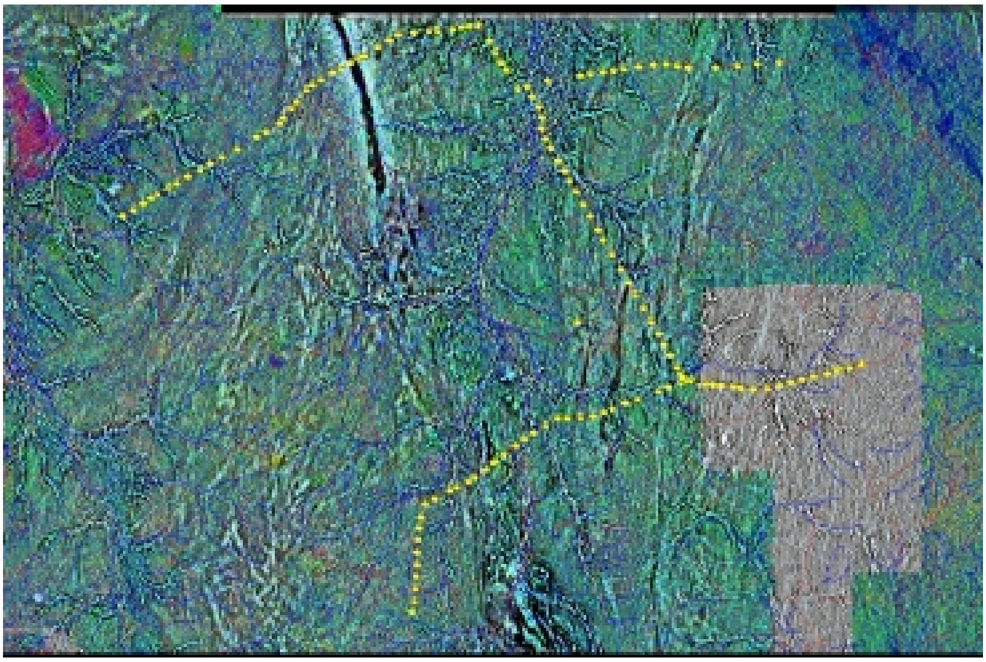

Figure 9. Combined radiometric and magnetic image of the Sussex-Coolabah area.

3.1.4 *Digital Elevation Model*

The digital elevation model was used as a basis for the production of 3D models and cross-section profiles. The remotely sensed data was manipulated and interrogated, which was achieved through the production of 3D models using ERDAS Imagine 8.4. The models incorporated all remotely sensed imagery and drill hole site locations. Two models were produced for each remotely sensed image including views facing south and north, with a vertical exaggeration of 20. The total count, single bands K and Th and 3 band colour composite radiometrics images (displayed as Red, Green, Blue), magnetics 1.5VD, and magnetics 1.5VD and KThU combined images were all used, producing a total number of 12 models.

A series of cross-sections was produced from deriving detailed elevation information directly from the DEM. The values were obtained and plotted out on three transects (along the Booroomugga, Coolabah and Elmore Roads) thus allowing accurate cross-sections to be produced. No DEM was available over the eastern end of Booroomugga transect, so the profile here was based on extrapolation from the height of surveyed drill hole collars.

The 1.5VD magnetics image draped over the DEM shows that the palaeovalleys containing magnetic sediments are mostly present in the lowest parts of the landscape. The image also highlights that some tributaries of the palaeovalleys have been partially topographically inverted, and are now located on the sides of hills (Figure 10).

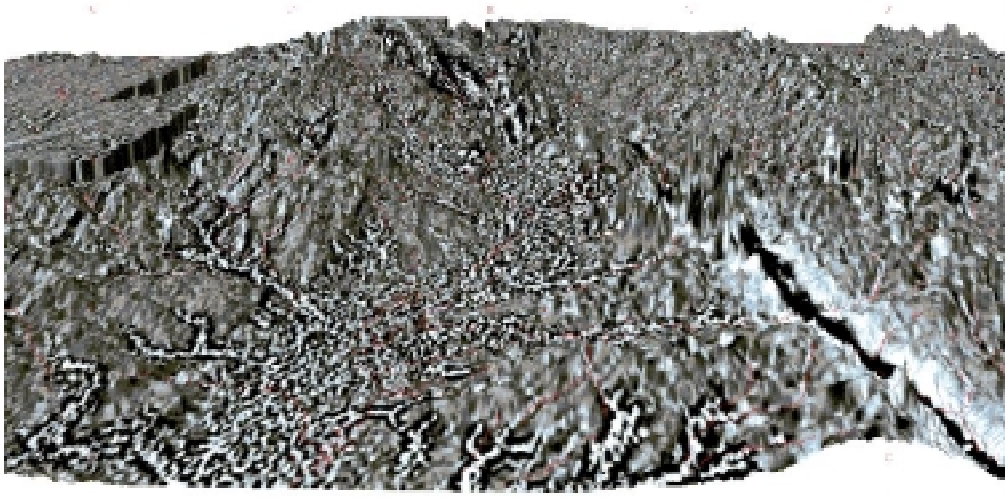

Figure 10. Airborne 1.5VD magnetic image drapped over DEM. View from north (foreground) to south (background).

3.2 Regolith Landforms

Regolith-Landform Units (RLUs) form the basis of regolith mapping, and were used in the construction of the Sussex-Coolabah 1:100,000 regolith-landform map over the eastern part of the study area (see back of hardcopy report). The regolith-landforms over the western part of the study area have been mapped by M. Spry as part of the 1:250,000 Cobar sheet for her current PhD studies. RLUs provide a description of the relationship between regolith types and their landscape setting. Regolith and landform types are described using a code system, which has specific letter combinations conveying the general information for each RLU (Pain *et al.*, in press). For example, CHep1:

- The upper case letters (CH) describe the main regolith type, (which in this case represent sheetflow deposits);
- The lower case letters (ep) describe the main landform type (which in this case represent an erosional plain);
- The modifier (1) is added to represent subtle differences within each RLU (for example surface lag type, such as angular quartz clasts).

The regolith-landform map for the eastern part of the study area was produced at 1:100,000 scale and comprises ten regolith-landform units which encompass alluvial, colluvial, erosional and depositional units (see regolith map). The regolith-landform units are as follows:

- ACa – Sub-rounded to sub-angular sands, silts and gravels, composed of quartz and lithic fragments within ephemeral meandering channels.

- Aap – Sub-rounded to sub-angular sands, silts and gravels, composed of quartz and lithic fragments in low relief areas.

- Apd – Sub-rounded to angular quartzose and lithic sands, silts and minor gravels within low relief areas.

- Aed – Sub-rounded to sub-angular quartzose and lithic sands and occasional gravels within depressions containing minor channels.

- Cep – Angular, lithic gravels mantling and flanking areas with slight relief.

- CHer – Angular to sub-rounded lithic and quartzose sands and gravels mantling and flanking areas with moderate relief. Surface materials consist of coarse lithic and quartz sand and gravel lags with occasional maghemite and red-brown silt size material.

- CHep1 – Sub-rounded to sub-angular lithic and quartz sands and gravels within low relief areas.

- CHpd – Sub-angular to sub-rounded lithic and quartz sands and gravels within low relief areas. Surface lag consists of fine lithic and quartz sand and gravel with occasional maghemite and red-brown silt size material.

- SMer – moderately weathered saprolite in areas of moderate topographic relief.

- CHep2 - Sub-rounded to sub-angular lithic and quartz sands and gravels within low relief areas. Highlighted by areas of increased alluvial incision.

3.3 Aeolian Sediments

The regolith geology of the Cobar-Girilambone district of NSW consists of transported regolith materials over *in situ* weathered bedrock. The transported regolith usually consists of a mixture of alluvial, colluvial and aeolian sediments. Furthermore, the alluvial, colluvial and aeolian components may also have particular types of composition. For example, aeolian sediments commonly consist largely of silt-and sand-size clay microaggregates, as well as silt-size quartz grains. In studying transported materials, it is critical to understand both their origin, ie. whether they are alluvial, colluvial, or aeolian, as well as their detailed physio-chemical properties.

Aeolian deposits can cause problems with the remote sensing of regolith materials. For example, radiometric data are frequently used to map regolith materials; however, the presence of aeolian dust in the regolith, can confuse the radiometric signature of the bedrock, masking the underlying geology. During geochemical surveys, the aeolian component, which may form a discrete mantle or be mixed into an existing profile, can dilute or mask geochemical expressions. Masking occurs where the aeolian component is abundant, giving a geochemical response unrelated to the underlying regolith profile and bedrock. Dilution reduces the magnitude of the underlying geochemical signature, for example gold and base metal anomalies (Dickson and Scott 1998, Scott 1999).

In addition to causing problems in exploration, the properties of aeolian sediments, in particular the stability of their clay microaggregates, can have significant effects on a range of landscape processes and hence have major implications for land management. For example, if the clay microaggregates present in these sediments are highly unstable and disperse into < 2μm particles, the soil profiles containing these materials will be highly prone to land degradation such as soil erosion (gullying, piping and rilling), poor air quality, and surface sealing, crusting and hardsetting problems (Greene et al. 2001).

The work outlined in this report is part of a larger study by the author (RSBG) who is investigating the properties of aeolian materials in southeastern Australia. This larger study aims to develop methods for recognising aeolian materials in the landscape, as well as understanding the stability of the clay microaggregates in aeolian materials. The author used the opportunity of the drilling program by NSW DMR in the Sussex area to obtain samples of possible aeolian origin.

The study site for the samples was in the general area of the transects used for the NSW DMR drilling program. Three samples of surface soil (0-10 cm) were taken on 3rd March 2001, from the following locations:

(i) 'El-Capitan'; an outcrop of basalt with a shallow (≤ 10 cm) layer of soil overlying undecomposed basalt.

(ii) CBAC19; a current drainage line of gravel alluvium.

(iii) CBAC16; a residual area of clay alluvium.

The methods of analysis were:
- The following determinations were carried out on the < 2mm fraction;
- Particle size analysis according to the method of Loveday (1974).
- pH and electrical conductivity (EC) 1:5 soil-water extracts.
- Exchangeable cation composition and exchangeable sodium percentage (ESP), using a 1M ammonium acetate, pH 7, extract.
- % Clay dispersion following end-over-end shaking for 1 hour of 1:5 soil-water extracts (Rengasamy et al 1984).
- XRD analysis for clay mineralogy was carried out on clay (< 2 μm) separates.

The results in Tables 2 and 3 illustrate the physical and chemical (including mineralogy) properties respectively of the three surface soils.

The main differences in particle size between the three samples are the higher clay content of CBAC16 compared with CBAC19 and 'El-Capitan', and the low amount of coarse sand in the El-Capitan sample relative to CBAC19 and CBAC 16 (Table 2).

Table 3 shows that the clay fraction of all three samples have similar mineralogy's, ie they all mainly contain illite and kaolinite. All three soils also have low levels of salinity (EC < 0 2 dS/m) and ESP. The amount of clay dispersion is also very low in all samples (< 3%).

When the ESP/EC values are plotted on the Rengasamy et al. (1984) diagram (used to identify dispersive soils), they are in the region of potentially dispersive (unpublished data). However, the low % clay dispersion values indicate that the clays in these soils are strongly aggregated, and resist mechanical breakdown in water.

Table 2: Particle size analysis of surface soils

Sample (0-10 cm)	**Particle size (%)** <2µm	2-20µm	20-60µm	60-200µm	0.2-2.0 mm
'El Capitan'	26	13	27	30	3
CBAC 19	22	12	15	29	22
CBAC 16	41	8	21	23	10

Table 2: Chemical (and mineralogical) properties of surface soils

Sample (0-10 cm)	**Mineralogy**	**EC (dS/m)**	**ESP**	**(%) Clay Dispersion**
El Capitan	Illite/kaolinite	0.14	0.6	1.8
CBAC 19	Illite/kaolinite	0.05	0	2.5
CBAC 16	Illite/kaolinite	0.04	0.7	1.2

The proposed model for modern, major dust-transporting wind systems (Sprigg 1982) indicates that the study area is likely to have an input of aeolian materials. However, the Cobar land systems map of Walker (1991), which includes the study site, shows that no aeolian features are recorded. The results of the particle size analyses in the current study indicate that the surface soils contain significant amounts of clay materials (Table 2) and that these materials appear to be strongly aggregated in water (Table 3).

The occurrence of strongly aggregated aeolian clays in the Australian landscape was first suggested by Butler (1956), who used the term 'parna' to describe clay materials which are transported by wind action and consist of stable microaggregates of silt and sand-size. Earlier work by Greene and Nettleton (1995) has shown these aeolian materials exist in land systems approximately 100 km west of the study site.

The data on a limited number of surface soil samples from the study area indicate the presence of stable microaggregates of clay material. These microaggregates still exist, even though pedogenic processes may have partly broken down the bonding in these clay materials. It is probable that this material was transported as aeolian dust. Further work on deeper samples from a range of depths in the B and B/C horizons is necessary to confirm these results.

3.4 Magnetic Palaeovalley Sediments

The 1.5 vertical derivative (VD) image of the airborne magnetic data displays an extensive network of magnetic palaeovalley sediments (Fig. 11) that, in general, broadly relates to present day valley sediments. In detail, however, present drainage sediments weave in and out over underlying magnetic palaeosediments. From other studies, maghemite is the likely magnetic mineral contained in these sediments. Modern alluvial sediments and eroding and depositing colluvial sheet wash mostly cover the magnetic palaeosediments, for example, along the north flowing stream in the central part of the study area, Mulga Creek, and its tributaries. There are limited areas of surface magnetic lag overlying palaeovalley sediments, as indicated by radiometrics (high thorium, low potassium, teal colour on 3 band composite image), mainly adjacent to Mulga Creek.

The airborne magnetics image displays the present extent of preserved magnetic palaeosediments. Modern sediments overlie these palaeosediments in places, and their radiometric signature masks that (high thorium and low potassium) of the surface exposures of the magnetic palaeosediments along Mulga Creek. From inspection of the regolith profile sections interpreted from drill hole logging (see section below) preserved palaeosediments are more extensive than the magnetic palaeosediments as indicated by the 1.5VD airborne magnetics image. Thus, preserved palaeosediments include less magnetic and/or non magnetic sediments. The palaeodrainage divides for the presently preserved magnetic palaeosediments are similar to the present drainage divides, with one weaving in and out of the other (Fig. 11).

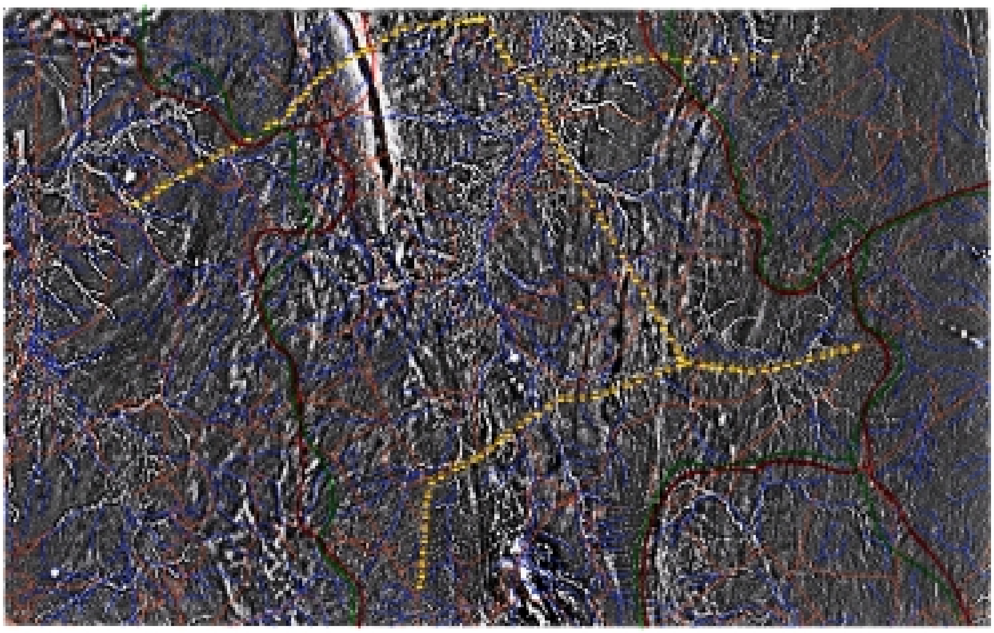

Figure 11. Enhanced airborne magnetic image showing a drainage network of magnetic palaeosediments. Palaeodrainage divides are shown in green and present drainage divides are shown in red. Present drainage is in blue, roads in dotted red, and drill holes in yellow.

In regolith landform unit CHep1 around the eastern end of the Booroomugga Road drill hole traverse present drainage sediments are less extensive than palaeovalley sediments. Limited stream incision along trunk tributaries occurred due to longer stream profiles and lower stream gradients on this plateau since sheet wash sediments infilled the palaeovalleys. In contrast, present drainage sediments are more extensive than magnetic palaeovalley sediments in regolith landform unit CHep2 surrounding CHep1. Increased stream incision due to shorter stream profiles and steeper stream gradients is eroding the CHep2 plateau by headward erosion and forming a scarp between the two units.

3.5 Drill Hole Logging

A standard set of drill hole log sheets combining requirements from both CRC LEME and NSWDMR, was produced. The logging sheets contain site, drill hole and interval information, lithological description, sample details, comments and regolith requirements (*eg*. landform, vegetation and weathering information). The 138 field logs are reproduced in Appendix 1a, GS2001/200.

Upon returning from the field, 33 drill hole samples were logged in more detail (Appendix 1) to incorporate common minerals, colour, texture, alteration and oxidation, through the use of a polarising binocular microscope (Wild Photomakroskop M400). The carbonate content for each of the selected holes was also tested, using concentrated HCl.

The 33 holes chosen from the total of 138 holes were selected as a representation of the materials found in the Cobar-Girilambone area. These holes were divided into palaeovalley and non-palaeovalley holes based on the following criteria:

Non Palaeovalley holes	Palaeovalley holes
Lithology	Present Landscape Position
Bedrock Alteration	Depth and Channel Morphology
Weathering (depth/type)	Sediment Composition
Landscape Position	Underlying Weathering
Geochemistry	

The detailed logging enabled correlations to be made with PIMA results, including definition of the transported/saprolite boundary, and context for correlation with geochemistry. Following the detailed logging of selected holes regolith units for the 138 holes were determined based on the dominant regolith material (*ie*. sand, clay, and gravel). Comparison between adjacent holes was used to construct a 3D-regolith architecture and to interpret of the landscape evolution for the Sussex-Coolabah area (see later sections of this report).

Drill hole samples were collected at every metre for the first 12 metres, then every two metres thereafter. Chip tray samples were taken at every possible interval, whilst samples for geochemical analysis (approximately 4 kg) were taken every metre for the first 12 and then collected every three metres until end of hole.

Each drill hole was photographed using a Nikkon E950 Digital camera back in the laboratory, and displayed in Adobe Photoshop. The holes were photographed, where possible, in consecutive order to compare samples between holes. The photographs are reproduced in Appendix 1c, GS2001/200.
Logging of 33 selected drill holes in detail enabled the determination of a transported/saprolite boundary; discrimination between the lithology/mineralogy of transported materials, changes in saprolitic lithology/mineralogy and the detection of regolith carbonate.

The transported/saprolite boundary for the 33 holes examined varied according to changes in bedrock lithology, landscape position and the presence of palaeovalleys. In the study area, the depth of this boundary changed markedly from an average depths for bedrock dominated holes at around 1-3 m, to an average depth of 25-30 m for palaeovalleys dominated holes. A full list of the transported/saprolite boundaries can be seen in Appendix 3.

The lithology/mineralogy of the transported materials also varied throughout the study area. Within bedrock dominated holes, transported materials were commonly shallow (< 3m) and consisted of red/brown silt, sand and clay with minor sub-rounded quartz and magnetic granules to pebbles. Transported materials present within palaeovalley holes, however, were deeper and lithologically more varied. These transported materials consisted mainly of sands, grey clay, magnetic gravels, lithic gravels or a combination of all these materials.

Changes in bedrock lithology and mineral composition are not as varied within the transported sediments. The dominant lithology throughout the field area was siltstone to phyllite, with sandstone, shale and chert occurring as minor lithologies. In certain places, a saprolite was bleached consisting entirely of kaolinite with minor quartz veining. The bleached saprolite was prominent beneath transported palaeovalley sediments, however, it was also found overlying saprolite within five bedrock-dominated holes (CBAC 7, 41, 70, 114 and 124). Hole 114 is located on a north-south trending structure on the magnetics image, possibly evidence for preferential weathering of the saprolite in this hole.

Cementation or overprinting was common throughout many holes. A number of bedrock dominated holes contained silicified lithic chips such as holes CBAC 1, 43, 83, 97, and 120. The silicification is found at depths of between 2 and 10 m. Indurated chips are also present in the transported regolith, including silicified and ferruginous saprolite (siltstone and sandstone), and silicified sediment (holes CBAC 12, 18, 29, 31, 52, 73, 74, 75, 77, 78, 103, 105, and 106).

Carbonate treatment results (Appendix 2) indicate that carbonate is prominent within the study area, with only 1 hole out of forty containing no carbonate. Carbonate is abundant in the transported materials of palaeovalley holes particularly holes CBAC 73-78, and is prominent in the upper saprolite within bedrock dominated holes. XRD results show the occurrence of dolomite, but due to the nature of the carbonate testing there was no detection of dolomite in the samples.

3.5.1 Deviant Database

The location data from 138 drill holes and detailed regolith logging of 33 drill holes were entered into the AGSO-Regolith Database, DEVIANT. The location data was automatically downloaded into the Deviant Sites_table (Oracle) using Unix scripts.
The location data correspond to the drill holes' Field ID (CBAC's) and AGSO's ID (200170001 to 2001700138). The fields that the data were entered into AGSO's DEVIANT database are: easting, northing, surface latitude, surface longitude, datum, zone, projection, ellipsoid elevation, mean sea level elevation (AMSL), and path of well (sidetrack) (Figure 12).

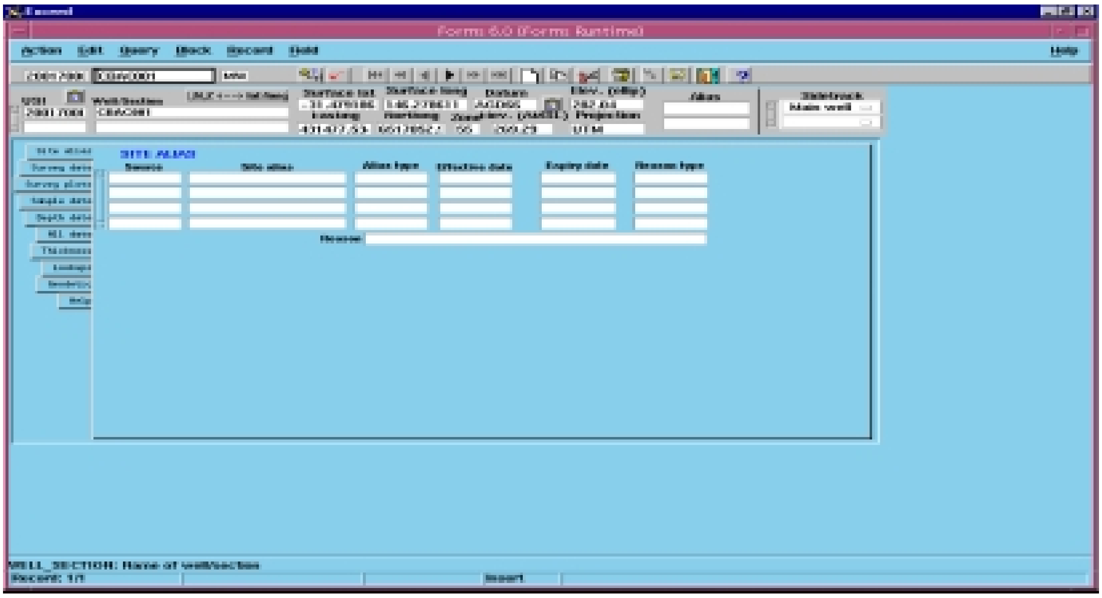

Figure 12. Deviant Site_table.

The drill holes location data was loaded into the Deviant database using two Unix scripts one for the Site_Location table (Figure 13) and one for Site_Sidetrack table (Figure 14).

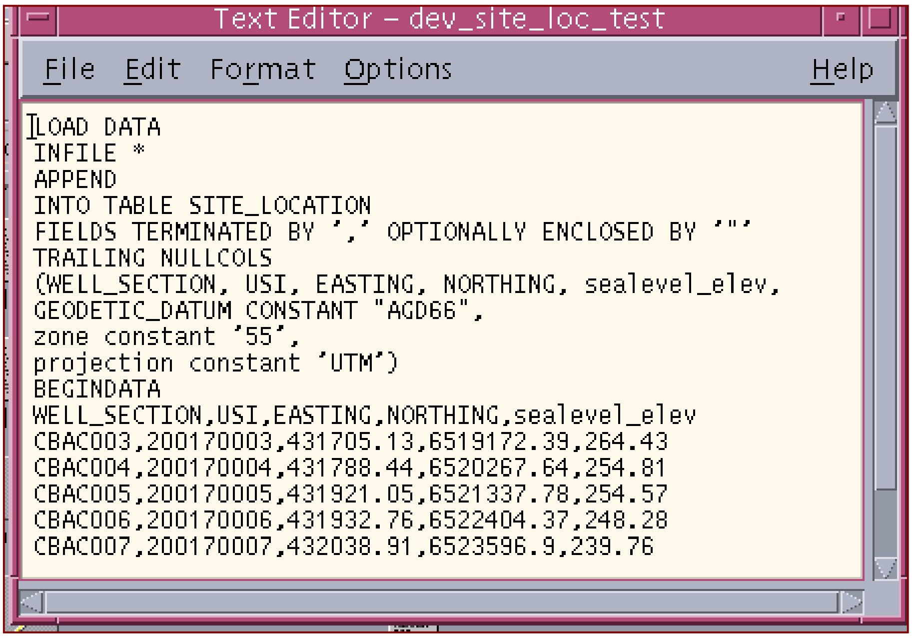


```
LOAD DATA
INFILE *
APPEND
INTO TABLE SITE_LOCATION
FIELDS TERMINATED BY ',' OPTIONALLY ENCLOSED BY '"'
TRAILING NULLCOLS
(WELL_SECTION, USI, EASTING, NORTHING, sealevel_elev,
GEODETIC_DATUM CONSTANT "AGD66",
zone constant '55',
projection constant 'UTM')
BEGINDATA
WELL_SECTION,USI,EASTING,NORTHING,sealevel_elev
CBAC003,200170003,431705.13,6519172.39,264.43
CBAC004,200170004,431788.44,6520267.64,254.81
CBAC005,200170005,431921.05,6521337.78,254.57
CBAC006,200170006,431932.76,6522404.37,248.28
CBAC007,200170007,432038.91,6523596.9,239.76
```

Figure 13. Unix script to load drill hole data in to Deviant's Site_Location table.

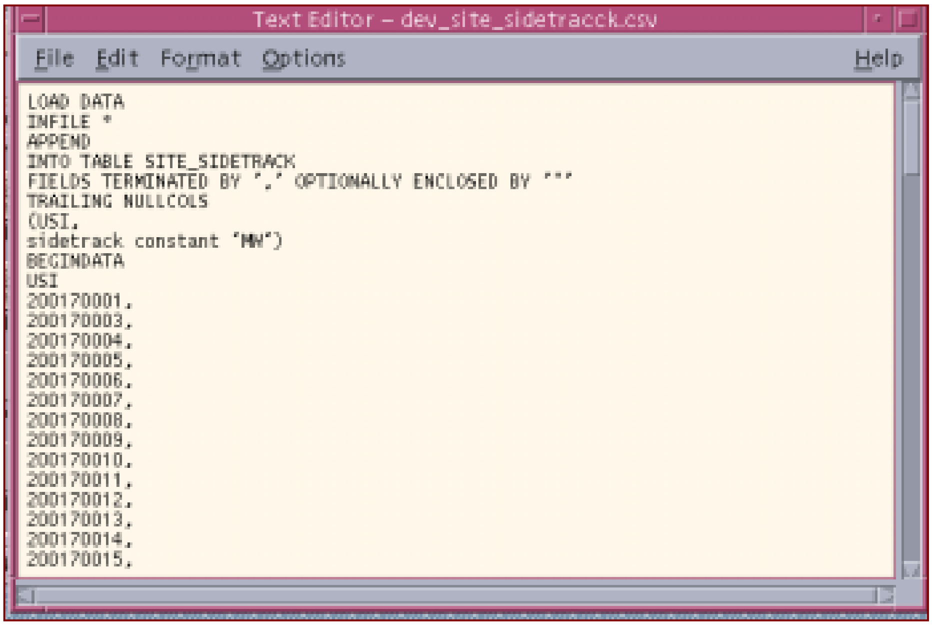

Figure 14. Unix script to load drill hole data in to Deviant's Site Sidetrack table.

The detailed regolith description (logging) data from 33 drill holes was entered by hand into the AGSO-Regolith Database, DEVIANT. The data was entered into two Deviant tables. Dip and azimuth of each drill hole were entered into the Survey_Data table (Figure 15) and detailed regolith description were entered into Depth_Data table (Figure 16)

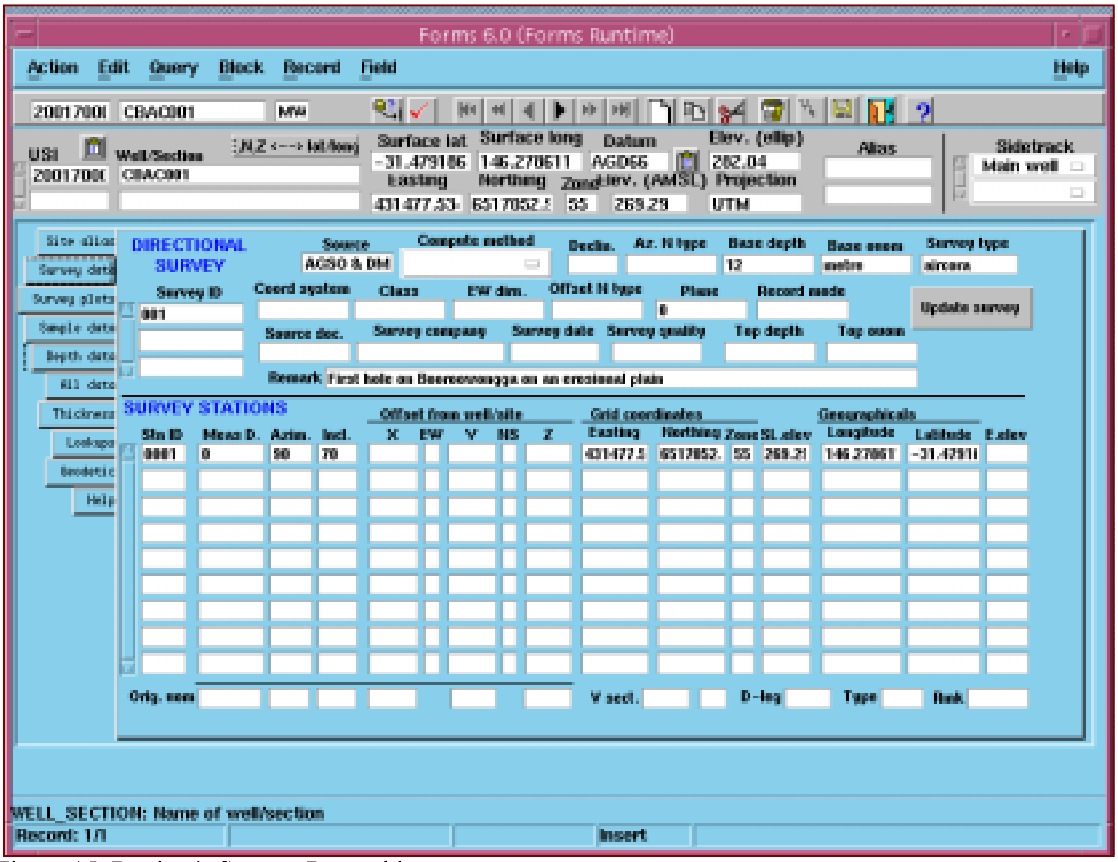

Figure 15. Deviant's Survey_Data table

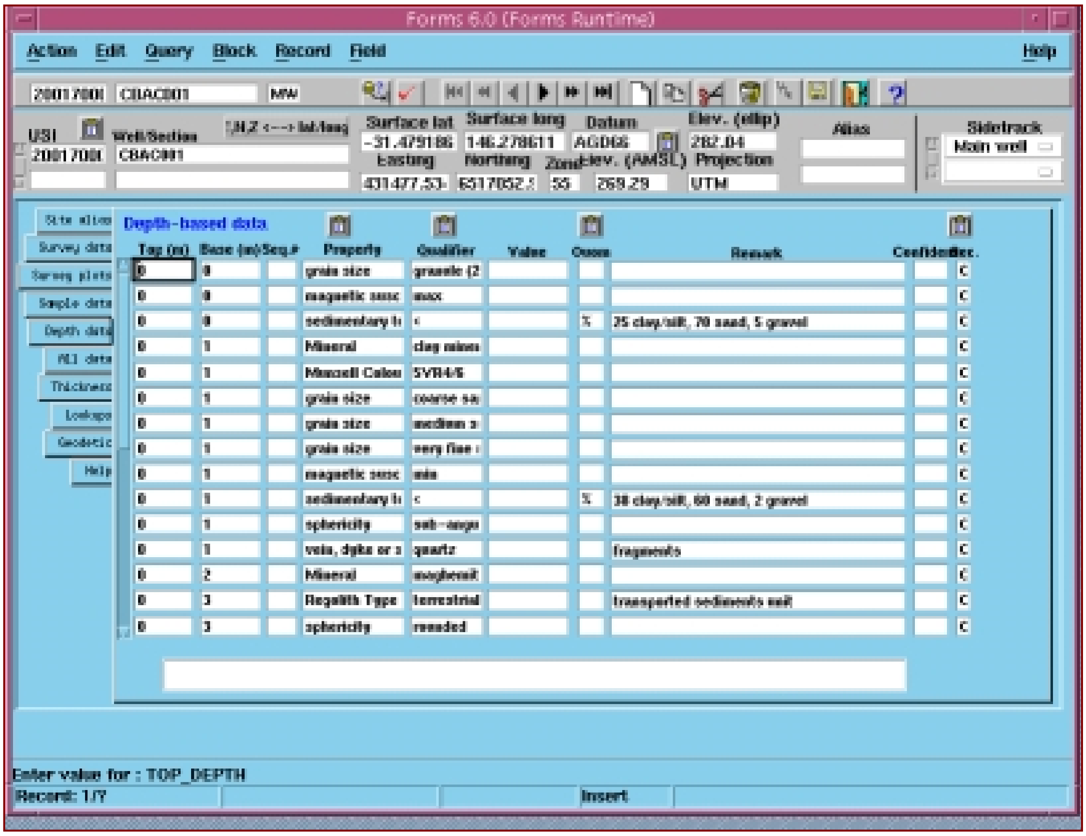

Figure 16. Deviant's Depth_Data table

3.6 PIMA Analysis

The Portable Infrared Mineral Analyser (PIMA) was used to analyse regolith materials from 42 representative drill holes. The aim of this study is to increase general information about the mineralogy, thickness and distribution of the transported sediments cover and *in situ* weathered bedrock (saprolite), and identify parent bedrock **lithology.** The materials were sampled at 1 and 2 metre intervals, and allowed to dry at room temperature prior to analysis.

Regolith drill hole materials were selected for analysis based on position in the landscape, geochemical significance, and presence of thick transported cover. The samples from 23 drill holes were analysed from the surface to the end of the hole. Samples from 18 drill holes were analysed to locate the unconformity (transported sediments / *in situ* boundary) and sampled 3-4 meters above and below the suspected unconformity zone. Drill hole numbers and their respective sample intervals that were analysed by PIMA are listed in the Table 4.

Table 4. Drill holes analysed with PIMA.

FIELD ID	AGSO site ID	PIMA samples ID	Sampled Interval (m)
CBAC001	200170001	P0001001 to 013	Surface - 12
CBAC004	200170004	P0004001 to 022	Surface - 22
CBAC010	200170010	P0010001 to 016	Surface - 16
CBAC012	200170012	P0012001 to 006	14 - 25
CBAC016	200170016	P0016001 to 020	Surface - 24
CBAC018	200170018	P0018001 to 024	Surface - 34
CBAC043	200170043	P0043001 to 013	Surface - 12
CBAC048	200170048	P0048001 to 006	12 - 24
CBAC049	200170049	P0049001 to 015	Surface to 16
CBAC051	200170051	P0051001 to 019	Surface to 24
CBAC052	200170052	P0052001 to 006	10 - 20
CBAC054	200170054	P0054001 to 028	Surface - 42
CBAC063	200170063	P0063001 to 019	Surface - 24
CBAC068	200170068	P0068001 to 006	Surface - 5
CBAC072	200170072	P0072001 to 010	11 - 30
CBAC073	200170073	P0073001 to 011	10 - 30
CBAC074	200170074	P0074001 to 005	18 - 26
CBAC075	200170075	P0075001 to 005	26 - 36
CBAC076	200170076	P0076001 to 028	Surface - 28
CBAC077	200170077	P0077001 to 005	26 - 36
CBAC078	200170078	P0078001 to 034	Surface - 54
CBAC080	200170080	P0080001 to028	Surface - 42
CBAC081	200170081	P0081001 to 017	Surface - 18
CBAC083	200170083	P0083001 to 013	Surface - 12
CBAC090	200170090	P0090001 to 011	Surface - 24
CBAC092	200170092	P0092001 to 011	18 - 40
CBAC095	200170095	P0095001 to 015	9 - 36
CBAC097	200170097	P0097001 to 016	Surface - 18
CBAC099	200170099	P0099001 to 027	Surface - 39
CBAC100	200170100	P0100001 to 005	2 - 7
CBAC102	200170102	P0102001 to 005	2 - 7
CBAC103	200170103	P0103001 to 008	14 - 30
CBAC104	200170104	P0104001 to 007	8 - 18
CBAC105	200170105	P0105001 to 022	Surface - 30
CBAC106	200170106	P0106001 to 006	9 -18
CBAC111	200170111	P0111001 to 006	Surface - 10
CBAC120	200170120	P0120001 to 004	Surface - 6
CBAC121	200170121	P0121001 to 013	Surface - 12
CBAC122	200170122	P0122001 to 009	Surface - 8
CBAC129	200170129	P0129001 to 021	Surface - 28
CBAC137	200170137	P0137001 to 006	9 -18
CBAC138	200170138	P0138001 to 008	14 - 30

The PIMA II spectrometer was used for all analyses. Spectral Geologist (TSG) version 2 computer package has been used in the presentation and interpretation of the PIMA data for this report. Spectral Geologist provides graphical interpretation by applying a series of algorithms to the spectra.

In these samples, 5 algorithms have been used to display downhole changes in the regolith profile. TSG scale has been applied to the algorithms to provide lateral correlation between drill holes. For this report, PIMA data is provided as stacked spectra and graphical interpretation as .DOC files and .TSG files.

3.6.1 Technical Background

The Portable Infrared Mineral Analyser is an instrument that uses Short Wavelength Infrared Light (SWIR) to illuminate a sample. The spectral absorption features observed in the PIMA spectra range from about 1300 nm to 2500 nm and are the result of combinations and overtones (harmonics) of fundamental lattice (mineral structure) vibrations that occur at longer wavelengths. These absorptions are the result of bending and stretching of molecules bonds. Crystallinity and bound/inter-layer water within a mineral structure influence the reflectance.

The bonds that give rise to absorption features in the SWIR include those in hydroxyl, water, carbonate and ammonia and between Al-OH, Mg-OH, and Fe-OH (Figure 17). These molecules are found as major components in phylossilicates (including clay, chlorite and serpentine minerals), hydroxylated silicates (such as epidotes and amphiboles), sulphates (alunite, jarosite and gypsum and carbonates.

Most minerals have a characteristic spectrum in the PIMA range (1300 -2500 nm) and can be identified by PIMA analysis. Most minerals also have diagnostic features between 2050 -2450 nm, and therefor can be grouped spectrally according to the wavelength position of the deepest absorption feature between 2050 - 2450 nm. In addition to mineral identification, the PIMA spectra can also provide information on the degree of crystallinity of a mineral. For example, clay minerals, such as muscovite, illite and kaolinite, display variations in the crystalline structure that may be detected spectrally, and which permit the delineation of temperature and chemical zoning in alteration systems or distinguish weathering from alteration related clays.

Spectral analysis with the PIMA can also be used to discriminate compositional variations within mineral groups. This is significant as mineral composition may vary systemically in an alteration system as a function of the temperature and composition of the altering fluids, and with proximity to zones of mineralisation, for example, illite → muscovite → phengite.

Many minerals have absorption features at the same wavelength, which overprint one another. Minerals such kaolinite, dickite and nacrite are separated only by minor absorption features. The spectra may also contain various degrees of noise caused by dark, opaque and/or magnetic minerals.

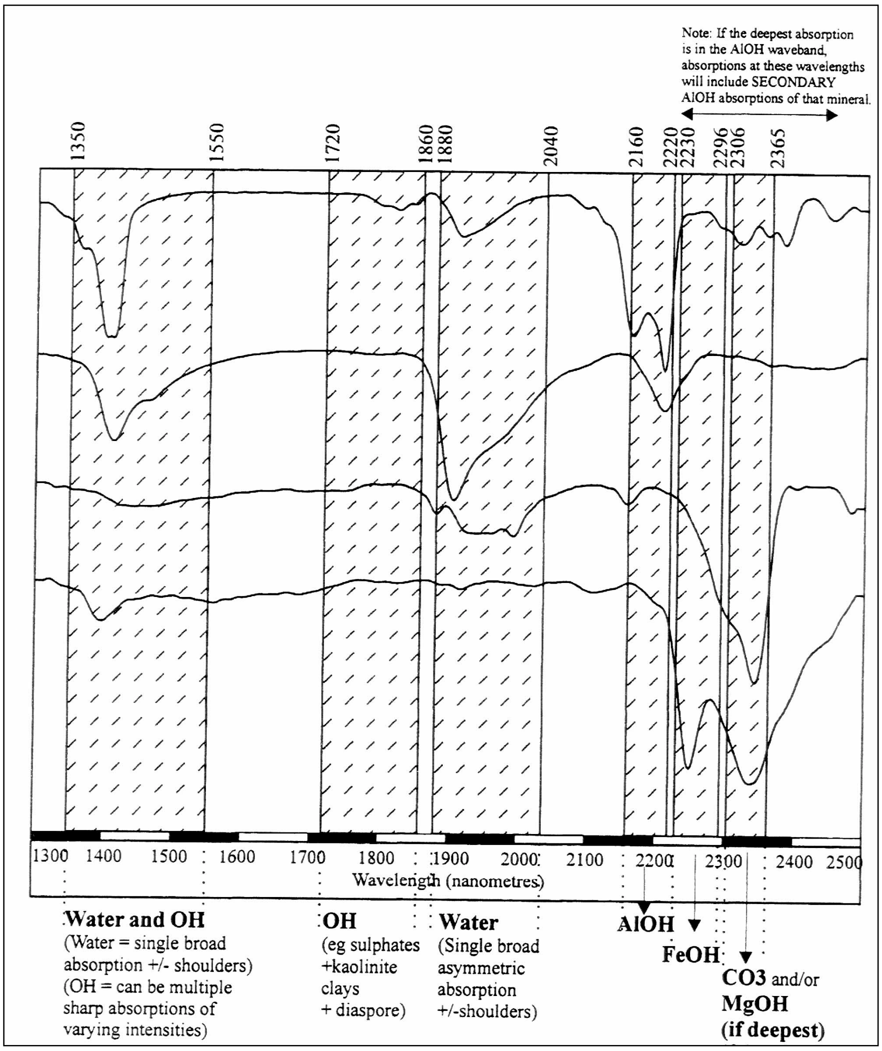

Figure 17. Major absorption features in the SWIR. The absorption features identified in this range are the hydroxyl, water, carbonate and ammonia bonds, as well as, Al-OH, Mg-OH, and Fe-OH bonds absorption features (Pontual et al, 1997).

3.6.2 *Methodology*

3.6.2.1 Recognising the Transported / Residual Boundary

An unconformity in a regolith profile is identified by the combined use of spectral changes, changes in kaolinite crystallinity and bound inter-layer water and clay mineralogy (Figure 18):

1. Contrast between spectra: transported sediments and *in situ* saprolite generally produce distinctive minerals with distinctive spectra;

2. Increase in kaolinite crystallinity in saprolite: transported kaolinite tends to have a disordered or poorly crystalline structure due to the transporting action, while *in situ* kaolinite has a more ordered or highly crystalline structure. The degree of kaolinite crystallinity (order) is observed at 2160-2180 nm region and can be calculated by taking the ratio between 2180 nm (disorder) and 2160 nm (order) (Figure 19).

3. Decrease in the bound inter-layer water absorption peak (1900-2000 nm): transported sediments tend to have more bound water in their minerals than *in situ* regolith.
4. Decrease in smectite content (may not occur in stripped profiles, beneath palaeovalleys or lake sediments).

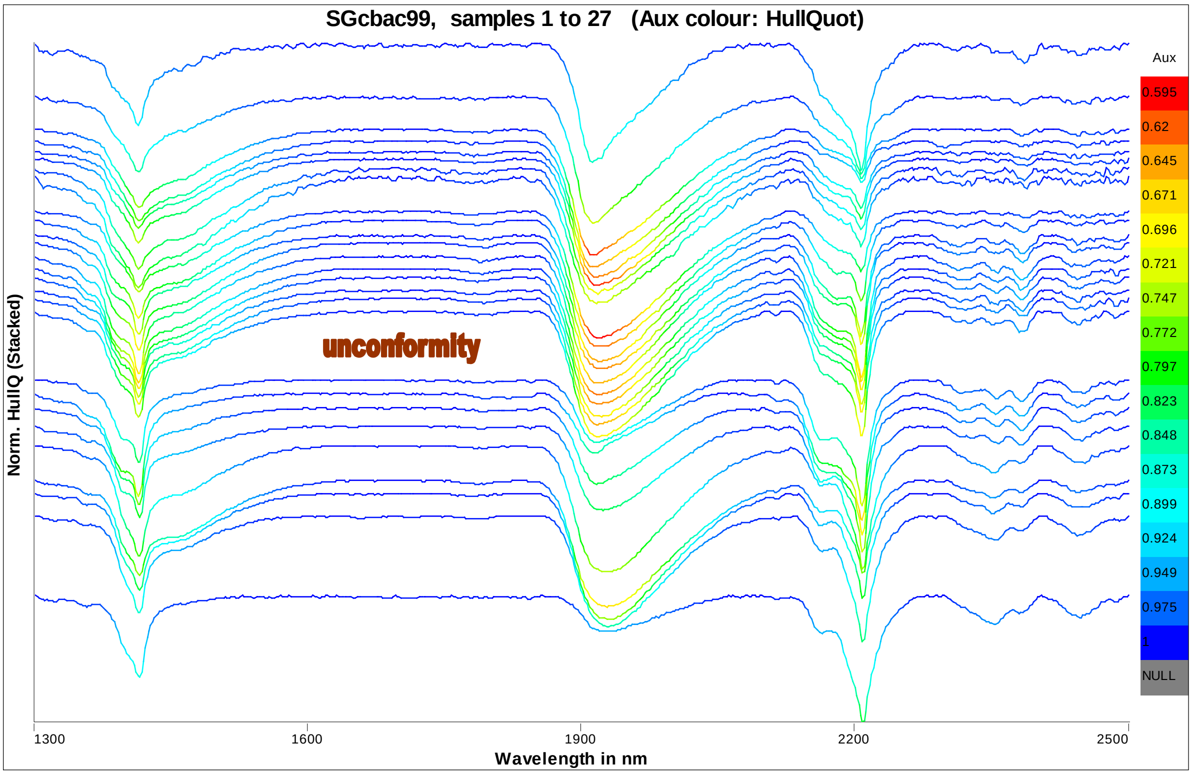

Figure 18. Spectral traces from CBAC 099. Palaeovalley sediments overlay saprolite, unconformity lies at 22 m deep. Red colour indicates deep absorption features; shallow absorption and background are represented in blue.

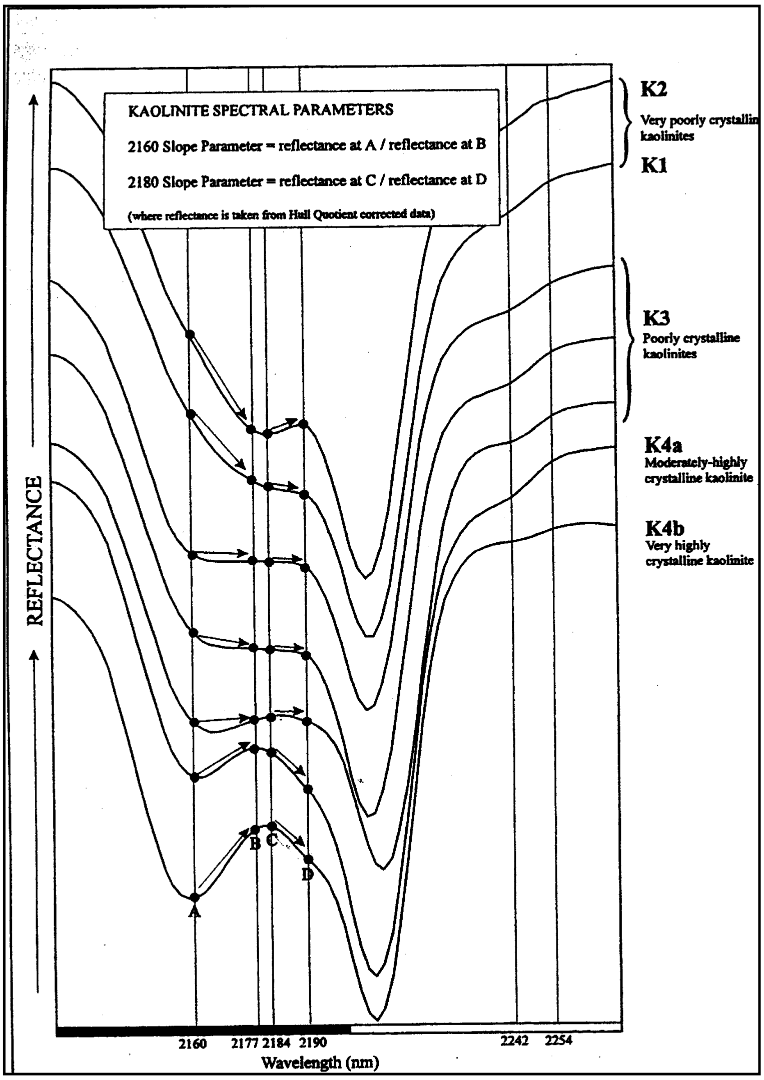

Figure 19. The degree of kaolinite crystallinity (order) is observed at 2160-2180 nm region and can be calculated by taking the ratio between 2180 nm (disorder) and 2160 nm (order).

3.6.2.2 Graphical Interpretation and Algorithms

3.6.2.2.1 Sample Numbers

Each layout represents a drill hole location and regolith profile. Each sample is numbered using an AGSO PIMA identification number: a standard P at the beginning, followed by three numbers corresponding to the drill hole number (eg. P001, P138), and the last three numbers corresponding to the sample interval (eg. CBAC 001). The surface sample PIMA identification number is P001001.

3.6.2.2.2 Hull Quotient and Colour Slicing

The degree of kaolinite crystalline disorder and the amount of bounded water in a mineral (-OH bond) influence the reflectance of the infrared radiation. Processing and enhancement of the spectral data involved the use of Hull Quotient technique to remove the background albedo effects.

Different colours reflect variations in absorption and depth. Deep absorption is shown in red, and shallow peaks and background are shown in blue. The bars in the histograms or logs represent the algorithm for a determinate sample. The length of the bars represents the algorithm increase or decrease. Colours in the histograms correlate to the depth variations of the major peaks (Hull Quotient).

3.6.2.2.3 Mineralogy

The mineralogy detected by PIMA is displayed in two columns, TSA Mineral 1 for the most abundant mineral and TSA Mineral 2 for the second most abundant mineral.

3.6.2.2.4 PIMA Algorithms

3.6.2.2.4.1 Water Peak

(1880-1960 nm).

The water peak indicates the presence of hydrated minerals (water within their crystalline structure).

3.6.2.2.4.2 Kaolinite Disorder (Crystallinity)

(2180/2160 nm).

Ordered kaolinite has an absorption feature at about 2160 nm, but with increasing disorder in the structure a feature at 2180 nm (reflecting the presence of "dickite domains") is developed.

3.6.2.2.4.3 Depth of the Fe-OH Peak

(2235 - 2245 nm).

This algorithm measures the relative depth of the absorption feature located in the range of 2235 nm to 2245 nm. The Fe-OH absorption feature is especially useful in regolith samples where kaolinite is dominant. This range highlights a small peak that can be related to the kaolinite absorption feature, and might be related to Fe substitution for octahedral Al within the kaolinite crystalline structure. Minerals such as montmorillonite and muscovite can overprint this feature, and therefore this algorithm works best when kaolinite is dominant.

In the saprolite this peak can be a good indicator of the original bedrock, whether rich in ferromagnesian minerals or not. Lack of iron in a saprolite derived from felsic bedrock results in little Fe substitution in kaolinite. Mafic bedrock will produce an iron rich soil and therefore a better developed Fe-OH peak feature.

3.6.2.2.4.4 Depth of the Al-OH Peak

(2180-2230nm)

This algorithm represents the aluminium hydroxide bearing minerals in the sample. The change in the depth and shape of this absorption feature represents different clays and tends to show changes in their crystallinity and quantity.

3.6.2.2.4.5 Wavelength of the Al-OH Peak

(2180-2230nm)

This algorithm measures the wavelength of the deepest point in the range 2180 to 2230 nm. A shift in the wavelength in this range signifies a change in mineralogy or variation in the composition of a single mineral.

This algorithm is useful in bedrock samples to determine changes in the composition of micas, ie between paragonite, muscovite and phengite. Paragonite has a wavelength approximately 2190 nm and is Na and Al rich. Muscovite has a wavelength of 2200 nm, which is often slightly decreased due Al content. Phengite has even less Al and therefore a longer wavelength of up to 2220 nm.

3.6.3 Regolith Mineralogy

The presence of kaolinite, montmorillonite, and illite, with minor halloysite, nacrite, and muscovite reflect transported sediments. Saprolite is mainly composed of quartz (not detected by PIMA), kaolinite and mica (muscovite and phengite). Nacrite and illite are also present in saprolite. The mineral occurrences in transported sediments and saprolite for the study area are documented in the

TSG mineral columns of the Spectral Geologist Profiles for the drill holes studied (available as digital data).

The minerals detected by PIMA in the Sussex-Coolabah regolith cover belong to 3 groups, kandites, illites, and smectites:

3.6.3.1 The Kandite Group

This group is made of kaolinite and its polymorphs, dickite and nacrite, and halloysite (hydrated kaolinite). These polymorphs have very similar crystalline and chemical structures, but their layers are stacked in different regular sequences. Absolute identification of dickite and nacrite requires further analysis of their PIMA spectral traces by correlation with X-ray diffraction. Therefore, these minerals are regarded as kaolinite in this report.
The kaolinite group of minerals includes the most common clay minerals. They are formed by the breakdown or weathering of feldspars, pyroxenes and other silicates or by hydrothermal alteration.

The Kandite Group.	
Kaolinite	$Al_4[Si_4O_{10}](OH)_8$
Dickite	$Al_4[Si_4O_{10}](OH)_8$
Nacrite	$Al_4[Si_4O_{10}](OH)_8$
Halloysite	$Al_4Si_4(OH)_8O_{10}8H_2O$

3.6.3.2 Illite/Muscovite Group

Illites are structurally related to micas. Illites differ from muscovite by having lower K content. They are often the dominant clay minerals in shales and mudstone, occurring also in sediments and soil. The weathering of muscovite can produce illite. Micas vary from Na-mica (paragonite) to the normal potassic variety (muscovite), and to Mg-Fe substituted mica (phengite)

The Illite / Muscovite Group.	
Illite	$(Ca_{0.1}Na_{0.06}K_{1.21})(Al_{3.06}Fe^{+3}{}_{0.44}Fe^{+2}{}_{0.06}Mg_{0.56})(Si_{6.8}Al_{1.2})O_{20}(OH)_4$
Muscovite	$K_2Al_4[Si_6Al_2O_{20}](OH,F)_4$

3.6.3.3 Smectite Group

Smectites are present in the study area as montmorillonite and nontronite. Smectites are structurally related to pyrophyllite except for the presence of water. They are known as swelling clays because of their capacity to take and hold water in their crystalline structure. Smectites are found in sediments that are derived from the weathering of basic rocks in poorly drained areas where magnesium is not leached. In good drainage conditions kaolinite is formed in place.

The Smectites Group.	
Montmorillonite	$({}_{1/2}Ca,Na)_{0.7}(Al,Mg,Fe)_4[(Si,Al)_8O_{20}](OH)_4.nH_2O$
Nontronite (Fe-rich smectite)	$({}_{1/2}Ca,Na)_{0.7}(Fe,Al,Mg)_4[(Si,Al)_8O_{20}](OH)_4.nH_2O$

3.6.4 *Analysis of Transported Sediments*

PIMA results help delineate the unconformity, and identify clay minerals in the transported regolith cover. Appendix 3 shows the base of the transported sediments for the drill hole materials analysed by PIMA. These depths result from the correlation of PIMA analyses with regolith materials descriptions (logging).

3.6.5 *Analyses of Saprolite*

(bedrock weathered *in situ*)

The study area is dominated by a saprolite derived from the weathering of mainly siltstones, but also sandstones, shales, and conglomerates. Fragments of weathered sedimentary bedrock and quartz can be found in the saprolite of almost all the studied drill holes. However, the PIMA analyses demonstrate that there are variations in the mineralogy of the country bedrock (sedimentary), with phengite and muscovite present in saprolite of some areas. There is also indication of weathered mafic intrusions, most probably mafic dykes.

3.6.5.1 Sedimentary Rock Saprolite

This saprolite is derived from the weathering of sedimentary rocks. The mineralogy identified by PIMA for saprolite derived from sedimentary bedrocks is kaolinite and its polymorphs (nacrite and dickite). The drill holes included in this category are CBAC 074 (18-26m), CBAC 106 (12-18m).

3.6.5.2 Sedimentary Rock Saprolite with Phengite and/or Muscovite.

Phengite, muscovite and slightly to moderately deformed and foliated fragments of the sedimentary rocks characterise this category. Four subdivisions may be defined by different degrees of weathering or primary mineralogy of the bedrock, these are:

1. <u>Saprolite with mica visible and phengite and muscovite detected by PIMA</u> (eg. CBAC 43, Figure 20).

The drill holes included in this category are: CBAC 001 (3-12m), CBAC 004 (1-12m, 20-30m), CBAC 010 (1-18m), CBAC 012 (18-25m), CBAC 043 (1-12m), CBAC 048 (18-24m), CBAC 052 (12-20m)

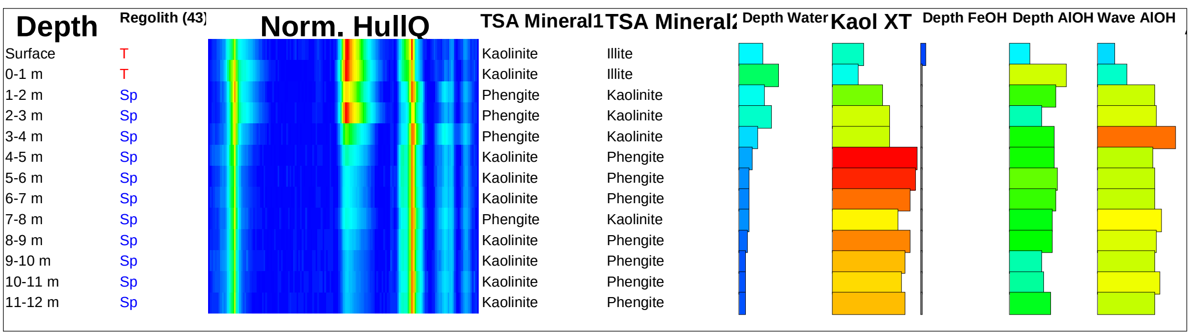

Figure 20. PIMA analyses of the regolith profile of drill hole CBAC 43. PIMA has detected phengite in saprolite; mica is visible in the logged regolith materials. The unconformity lies at 1 m.

2. Saprolite with mica visible and muscovite detected by PIMA (no phengite) (eg. CBAC 83, Figure 21).

Saprolite is mainly composed of muscovite and kaolinite, with some quartz veins. The drill holes included in this category are:

CBAC 049 (6-16m)
CBAC 054 (14-20m)
CBAC 004 (12-20m)
CBAC 010 (1-14m)
CBAC 049 (6-8m, 10-12m)
CBAC 063 (3-6m, 7-14m, 20-24m)
CBAC 063 (6-7m, 14-20m)
CBAC 073 (30-36m)
CBAC 075 (34-36 m)
CBAC 076 (20-24m)
CBAC 077 (32-36m)
CBAC 078 (52-54m)
CBAC 081 (5-8m, 11-18m)
CBAC 083 (10-11m)
CBAC 090 (18-24m)
CBAC 092 (22-40m)
CBAC 095 (22-36m)
CBAC 097 (1-11m, 12-18m)
CBAC 100 (6-7 m)
CBAC 102 (5-7m)
CBAC 103 (22-30m)
CBAC 121 (4-12m)
CBAC 122 (2-8m)
CBAC 129 (24-28m)
CBAC 137 (12-18m)
CBAC 18 (20-34m)
CBAC 76 (30-36m)
CBAC 83 (10-12m)
CBAC 97 (11-12m)

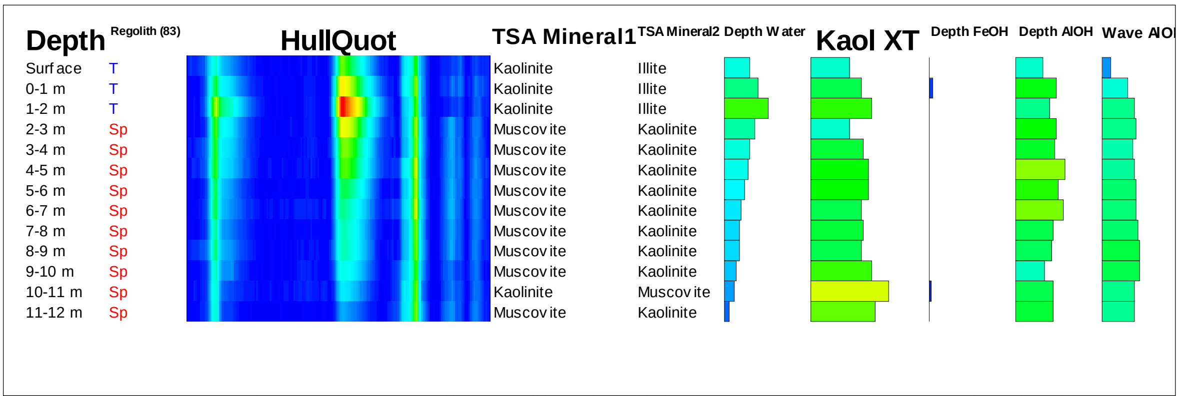

Figure 21. PIMA analyses of the regolith profile of drill hole CBAC 83. The unconformity lies at 2 m. Muscovite is detected by PIMA alone from 2 to 10 m, but muscovite is detected by PIMA and is also visible with logging from 10 to 12 m.

3. <u>Muscovite only detected by the PIMA</u>.

The drill holes included in this category are:

CBAC 83 (2-10m) (Figure 21)
CBAC 051 (14-24m)
CBAC 054 (20-42m)
CBAC 068 (3-5m)
CBAC 072 (16-30m)
CBAC 083 (2-10m)
CBAC 104 (11-12m, 16-18m)
CBAC 105 (16-26m, 28-30m)

3.6.5.3 Mafic Bedrock Saprolite

Phengite or muscovite is not present in this saprolite. Kaolinite is the dominant clay mineral, as the weathering of mafic rocks tends to produce large amounts of kaolinite. The kaolinite intervals display a deep absorption feature for the Fe-OH peak, which is an indication of ferromagnesian bedrock (ex. CBAC 016, Figure 22). The drill holes included in this category (see also 3.7.1.1 below) are:

CBAC 016 (8-24m)
CBAC 048 (16-18m)
CBAC 104 (12-16m)
CBAC 105 (26-28m)

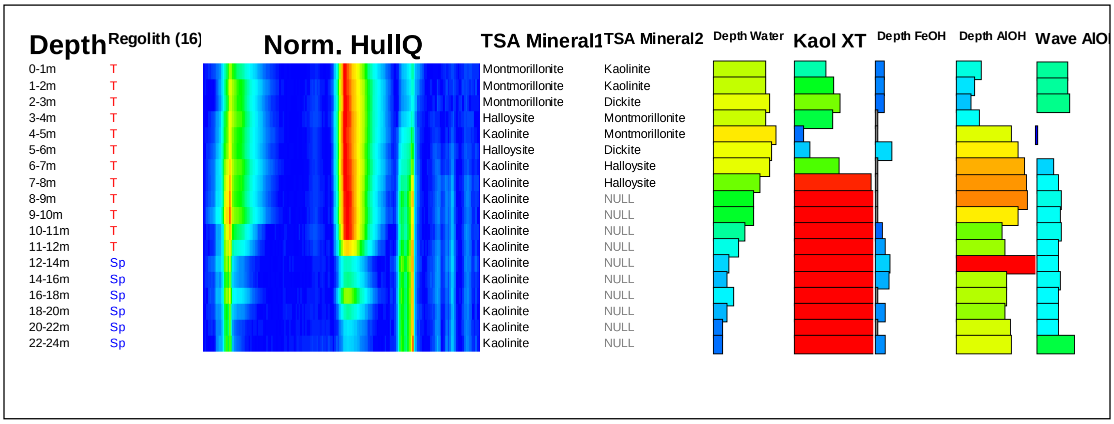

Figure 22. PIMA analyses of the regolith profile of drill hole CBAC 16. The unconformity lies at 12 m. In the saprolite highly crystalline kaolinite dominate, and the deep FeOH absorption peak indicates that the saprolite is derived from the weathering of a mafic dyke.

3.7 Regolith Geochemistry

Inspection of the geochemical data from the Sussex-Coolabah drilling program revealed that several profiles contain samples with anomalous levels of base metals (see also Fleming *et al.*, 2001). Ten of these profiles were selected for detailed investigation of their geochemistry relative to mineralogy in order to understand the significance of the geochemistry. Mineralogical data was provided by interpretation of the distribution of carbonate (as determined by HCl acid attack) and PIMA (and in some cases, X-ray Diffraction) traces.
\

3.7.1 *Profiles with Anomalous Base Metals*

3.7.1.1 High Cr

Chromium contents ≥200 ppm were observed in ten drill holes, CBAC 4, 10, 16, 29, 49, 76, 80, 99, 101 and 105. Because mafic dykes are known to occur in the Girilambone Group, high Cr intervals were suspected to reflect such dykes. Because the high Cr interval in drill holes CBAC 4 and CBAC 16 is within 4m composites, these were resampled at 2m intervals and Ti and Zr also determined in these samples. These additional results indicate that Ti is often >3% between 12 and 24 m in CBAC 16 where Cr is >200 ppm. The Ti/Zr ratios in this interval average 87 (suggestive of mafic rocks: Hallberg, 1984). Mineralogy determined by PIMA indicates the presence of kaolinite without associated muscovite (Figure 23). X-ray diffraction also indicates the strong development of kaolinite (with only trace or no muscovite) associated with goethite ± haematite and strong development of an alunite-jarosite mineral and rutile plus possible trace amounts of barite. Such a mineralogical assemblage is consistent with the presence of relatively low K contents (<0.45%) in this interval with elevated Ba (up to 0.88%), S (up to 0.42%, but not directly correlated with Ba) and Pb (>50 ppm).

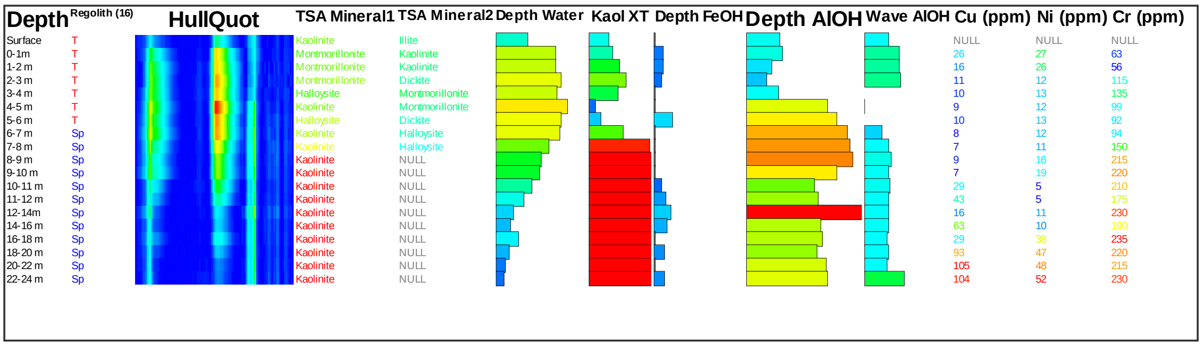

Figure 23. High Cr bearing mafic bedrock. profile in drill hole CBAC 16.

PIMA study also reveals that samples from CBAC 4 have kaolinite as the dominant clay mineral from 12 to 20 m (Figure 24) with Cr and Ti anomalous and K anomalously low (≤0.45%) in the interval 14-20 m. Ratios of Ti/Zr average 120 in the interval 16-20 m and 40 outside that interval. Thus intervals with elevated Cr and Ti but low K content appear to reflect weathered mafic rocks in the Sussex-Coolabah area. Such zones are readily seen in profiles derived by PIMA, which because of ease and speed is recommended as an efficient tool in delineating such mafic zones even when they are comparatively narrow.

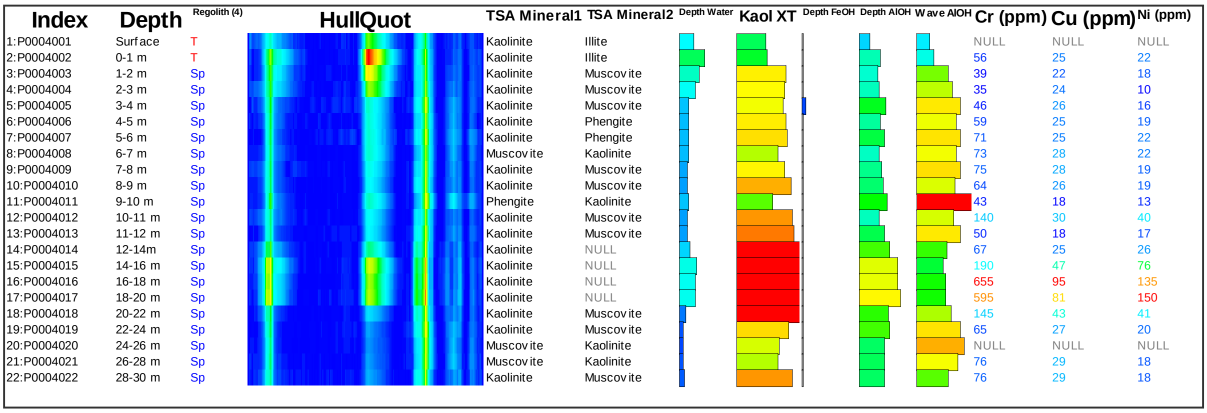

Figure 24. High Cr in the 12-20 m saprolitic kaolinite of drill hole CBAC 4.

3.7.1.2 *High Cu*

Greater than 200 ppm Cu occurs in the top 3 metres in CBAC 1 but such an interval is entirely within the transported material as identified by PIMA (Figure 25). Furthermore, although Zn~60 ppm may also occur with this Cu, elevated Cu contents are not accompanied by any other potential pathfinder elements (*eg.* As or Pb). Thus mineralisation would not be expected to occur directly below this interval, and only one slightly anomalous value Cu=100 ppm at 6-7 m is recorded. The anomaly in the transported material could imply local derivation although the strength of the anomaly (only 3 other Cu contents >200ppm were found during the whole drilling program) suggests that these values at the start of the program should be treated cautiously.

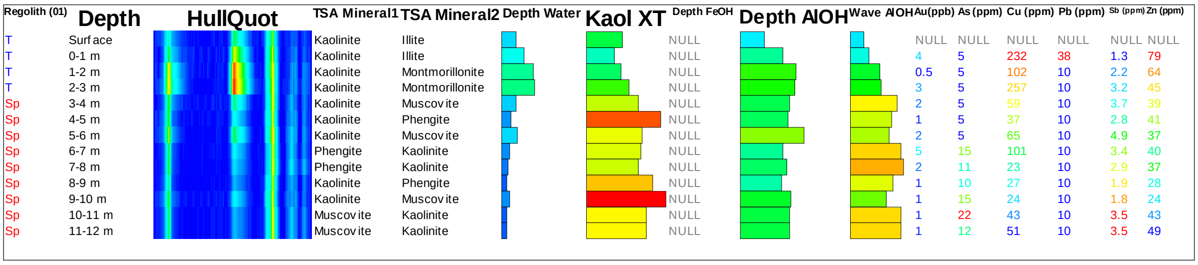

Figure 25. High Cu intervals in drill hole CBAC 1.

The highest Cu content found during this drilling program occurs in CBAC 121 at 2-3 m. Figure 26 shows that this sample is within residual saprolite but, although it contains 910 ppm S, no other chalcophile elements are present. Thus, with the lack of vertical extent of the anomalous Cu and lack of associated potential pathfinder elements, the anomaly should not be highly regarded. The anomaly occurs in the midst of a zone of carbonate (identified by HCl acid) which extends from 1 to 8 m, ie. well into the saprolite and it is possible that the alkaline conditions generated by the presence of carbonate may be responsible for stabilising the Cu here (*cf.* the similar retention of hydromorphically dispersed Cu and Zn in carbonate in the regolith at the Waterloo deposit, NE Queensland, Scott, 1997).

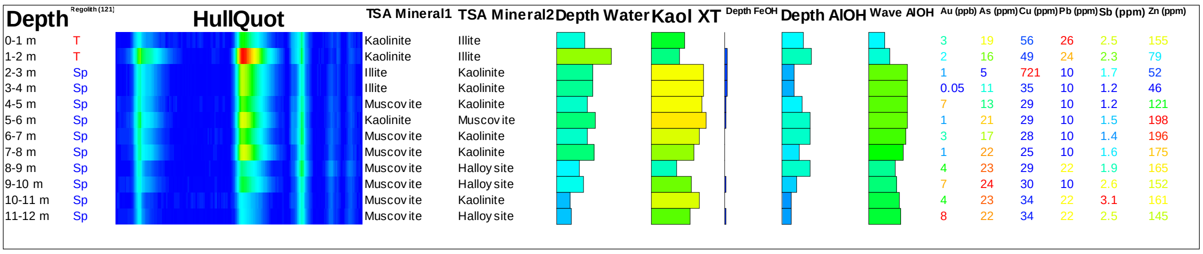

Figure 26. High Cu at 2-3m in saprolite in drill hole CBAC 121.

3.7.1.3 *High Zn*

Highly anomalous Zn occurs in the basal 12 m of drill hole CBAC 80 (Figure 27) became obvious during resampling. It is not accompanied by any other pathfinder elements. The extent of this anomalous Zn and the absence of Cu or Mn with it suggests that it should be investigated further, initially by XRD study.

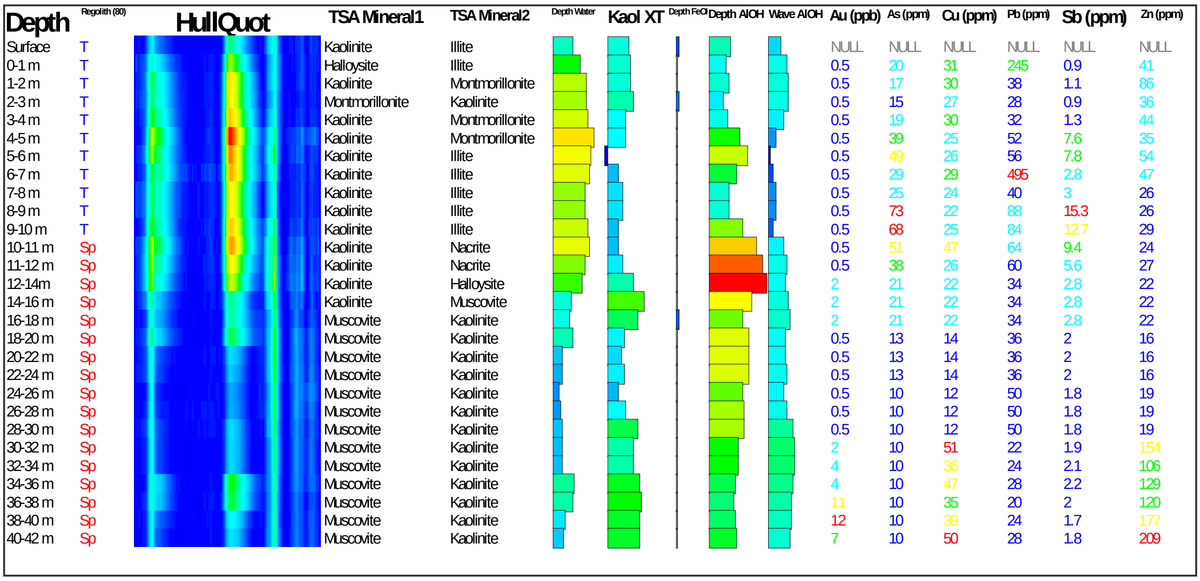

Figure 27. Highly anomalous Zn in the 36-42 m interval of drill hole CBAC 80.

The high Zn contents in the upper two samples in the next hole, CBAC 81, (Figure 28) could well represent cross hole contamination.

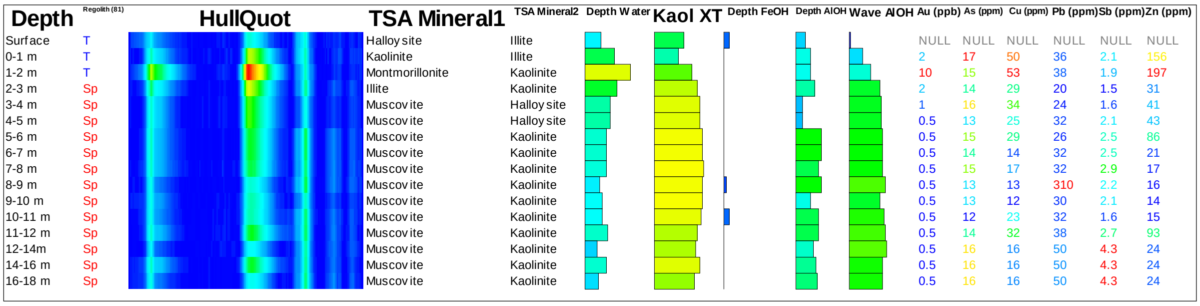

Figure 28. High Zn in the 0-2 m interval in drill hole CBAC 81.

3.7.1.4 *High Pb*

Lead contents >50 ppm occur from 7-24 m in CBAC 16. It has already been seen above that such an interval represents a mafic intrusion and contains a S-rich alunite-jarosite mineral and possible barite. The presence of elevated As, Sb and S with the Pb (Figures 29 and 30) suggests that this interval reflects weakly mineralised (probably dominantly pyrite) mafic rock.

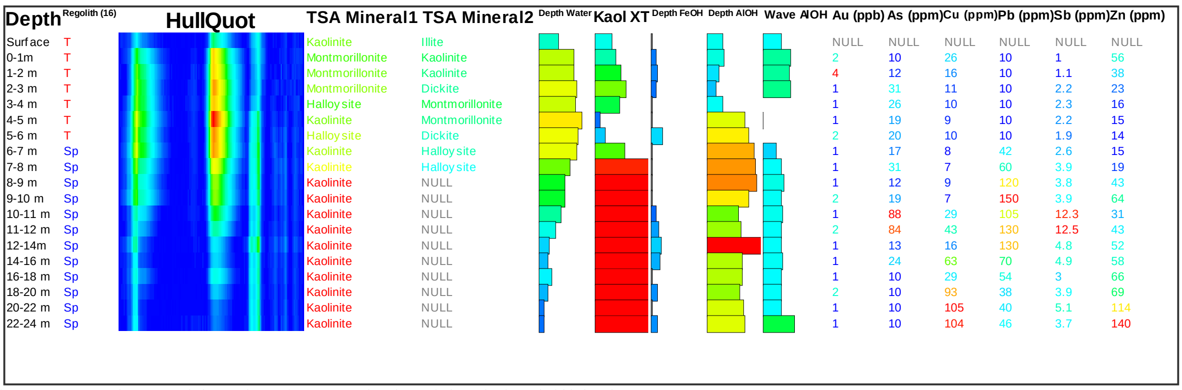

Figure 29. Elevated levels of As and Sb with Pb in drill hole CBAC 16.

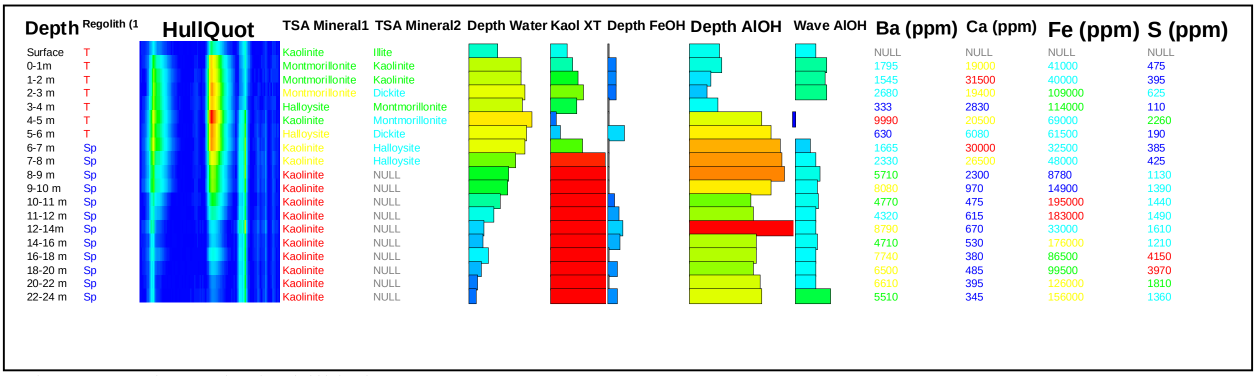

Figure 30. Elevated S in drill hole CBAC 16.

Drill hole CBAC 80 has As and Sb associated with anomalous Pb from 0-12 m. Such an association of pathfinders with the Pb adds confidence in regarding the anomaly as significant. However PIMA results clearly indicate that this interval is within transported material (Figure 27). Nevertheless, because of the retention of the pathfinder elements with the Pb, it is likely the anomaly consists of transported gossanous fragments and that their source is not too far distant.

The anomalous Pb in CBAC 43 occurs between 3 and 7 m *ie.* within residual saprolitic material (Figure 31). X-ray diffraction reveals an alunite-jarosite mineral to be present in this interval, although S is low (<100 ppm). Thus this alunite-jarosite mineral must be P- rather than S- rich. Thus, because it also lacks the associated pathfinder elements found in CBAC 16 and 80, this anomaly should probably be ranked as a lower follow-up priority than those with Pb plus As and Sb.

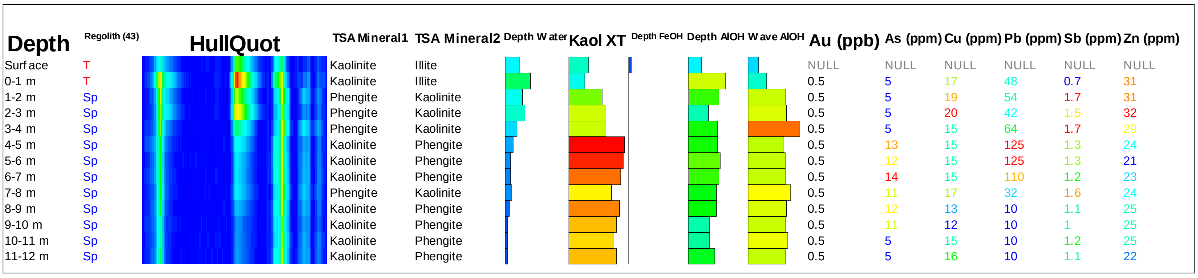

Figure 31. Anomalous Pb in drill hole CBAC 43 between 3 and 7 m within residual saprolitic material.

Anomalous Pb (=310 ppm) at 8-9 m in CBAC 81 occurs in residual saprolite (Figure 28) where XRD also reveals dolomite to be present. This sample has low S and chalcophile element contents. As in the case of stabilisation of anomalous Cu in CBAC 121 with carbonate (see above), this spot anomaly should be treated cautiously.

3.7.1.5 High Au

The most significant Au mineralisation occurs in CBAC 63 where Au >10 ppb occurs from 1- 20 m. Unfortunately this anomalous Au interval is not associated with any elevated chalcophile element contents *ie.* the Au is not accompanied by any pathfinder elements (like As or Pb) which could assist during exploration.

PIMA and detailed logging of the drill hole indicates that transported material occurs to 2 m depth (*eg.* Figure 32), so that the presence of anomalous Au in the saprolite appears to be reflected in the transported material. However Au is not anomalous in the surficial sample even though it contains some calcrete. Thus further understanding of the weathering processes occurring in this area is necessary if calcrete sampling is to be used in this region.

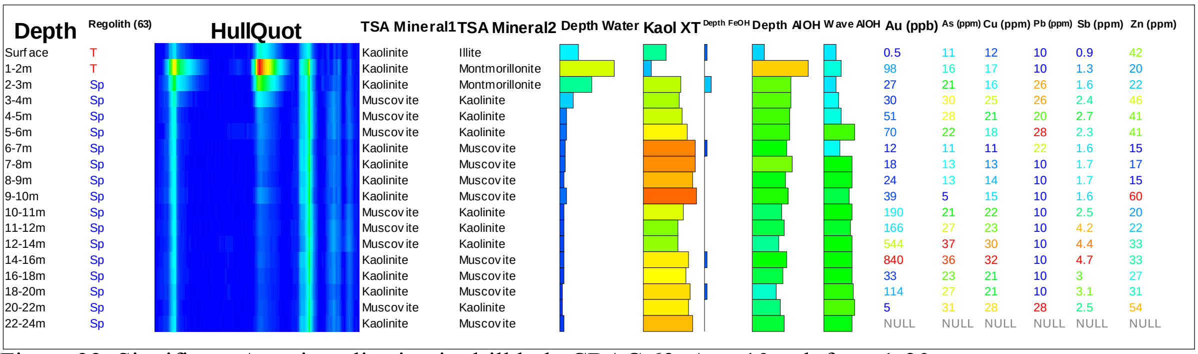

Figure 32. Significant Au mineralisation in drill hole CBAC 63, Au> 10 ppb from 1-20m.

The data set shows several cases where anomalous Au is present in the top few metres of a drill hole and where the basal sample of the preceding hole was also Au-bearing (*eg.* Table 5). In such cases it is possible that material from the anomalous interval in one hole has still been present in the drilling rig assembly and has been incorporated into material from the top few metres of the next drill hole.

Table 5. Possible cross contamination between drill holes CBAC118 and CBAC119.

Hole No	From (m)	To (m)	Au (ppb)	Al (ppm)	As (ppm)	Ca (ppm)	Cu (ppm)	Fe (ppm)
CBAC118	0	1	3	81000	14	27500	26	23500
CBAC118	1	2	4	101000	26	9310	39	47500
CBAC118	2	3	2	57500	10	600	26	34500
CBAC118	3	4	4	60000	14	5670	27	40000
CBAC118	4	5	3	89500	20	215	39	41000
CBAC118	5	6	16	73500	15	245	48	33500
CBAC119	0	1	19	59500	14	<50	43	35000
CBAC119	1	2	12	59500	15	<50	29	29500
CBAC119	2	3	2	91500	13	700	47	49500
CBAC119	3	4	7	104000	14	5810	40	44500
CBAC119	4	5	7	101000	17	6780	60	43500
CBAC119	5	6	9	102000	16	6450	54	46500
CBAC119	6	7	2	96500	14	2430	46	46500
CBAC119	7	8	4	110000	13	7210	43	43000
CBAC119	8	9	5	104000	12	115	40	44000
CBAC119	9	10	6	119000	14	180	75	38000

3.7.1.6 High Ba

The high Ba contents and accompanying S in drill hole CBAC 16 have already been commented upon above where Ba is suspected to be present both in an alunite-jarosite mineral and possibly some barite. However in some drill holes anomalous Ba occurs in intervals where S content is low *eg.* CBAC 97. In this profile, Ba >2200 ppm occurs from 4-12 m with S generally <300 ppm. In this drill hole, PIMA and logging indicate that the unconformity occurs at 1m (Figure 33) and HCl acid indicates calcite is also present in the transported material. XRD indicates that dolomite occurs with calcite in the top of the saprolite from 1-5 m and that an alunite-jarosite mineral is present in some samples from 3-7 m. These results suggest that such an alunitic mineral is a Ba- P- rich member of the series.

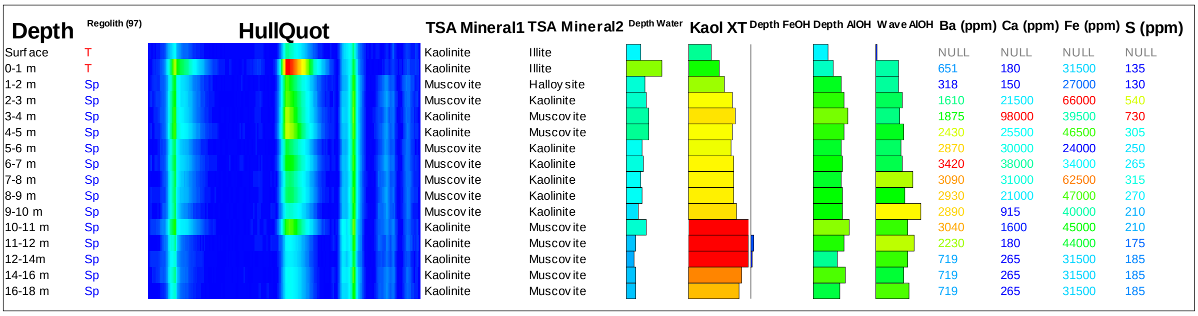

Figure 33. High Ba intervals (4-12m) in drill hole CBAC 97.

3.7.1.7 *High S*

In drill hole CBAC 83, S >2000 ppm with Ba <800 and Ca <600 ppm occurs at 10-12 m. Sulfur contents >500ppm, unaccompanied by significant Ba or Ca, occur up to 3m and 6m respectively. PIMA and logging indicate that the unconformity is at 2 m (Figure 34) and that calcrete occurs to 3m. XRD indicates that an alunitic mineral occurs in the sample from 11-12 m. No significant base metal contents are observed in this high S interval and thus it appears that it probably results from the weathering of pyrite which was poor in base metals *ie.* barren pyrite.

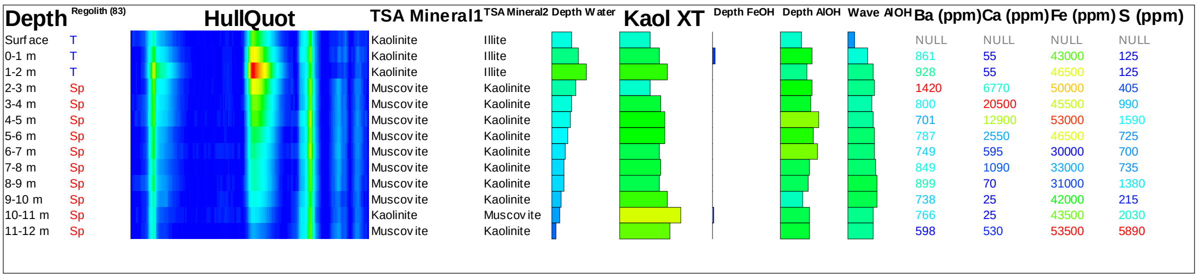

Figure 34. High S unrelated to Ba or Ca in drill hole CBAC 83.

3.7.2 *Implications for Exploration and Further Work*

Integration of mineralogical data determined by PIMA, XRD and HCl treatment with geochemical data has proved valuable in developing an understanding of the weathering processes, which have affected regolith samples from the Sussex-Coolabah drilling program. In particular, the recognition of mafic rocks within the profile initially by their high Cr and low K contents and then their ready detection by PIMA (as completely kaolinite-dominated samples) should prove useful during exploration, especially because such dykes may themselves be mineralised (as in the case of the mafic material in drill hole CBAC 16).

Knowing where the unconformity is, as obtained by PIMA (Appendix 3), specific geochemical anomalies can be placed in context *eg.* the Cu in CBAC 1 is seen to be in transported material.

The program of using PIMA to provide mineralogical data rapidly, along with specific more detailed mineralogical information by XRD, has proved effective in developing an understanding of the significance of geochemistry in this area. A similar work plan is recommended for future drilling. It may also be useful to do some further detailed mineralogical determinations to confirm postulated alunite-jarosite mineral compositions using an electron microprobe. Such minerals have often been found to stabilise normally mobile pathfinder elements like Cu and Zn in regolith samples (*eg.* Scott, 1987, Cairns *et al*., 2001)

3.8 Regolith Profile Sections

Regolith profiles were interpreted for each of the 138 drill holes based on microscopy and PIMA analyses where available, and field logs where not. These drill hole profiles were located on a vertically exaggerated land surface profile derived from the NSW DMR digital elevation model (flown by Tesla Airborne Geoscience as part of the DMR Discovery 2000 Initiative). Interpolated sections were derived from the drill hole profiles along the 3 traverses (in back of hardcopy report): Traverse 1 - Booroomugga Road (W-E); Traverse 2 - Elmore Road (SE-NW); and Traverse 3 - Coolabah Road (W-E). CBAC (Cobar air core) drill hole numbers are annotated with "L" for laboratory microscopy and "P" for PIMA where these analyses have been done. Points of inflection where the traverses change direction are indicated with true north arrows. Regolith landform types are annotated along the section profiles. Transported, mixed provenance and *in situ* regolith types are distinguished (see legend), with the transported-saprolite boundary highlighted (see definition (Eggleton, 2001) of "saprolite" in appendix). Induration modifiers, and clasts/fragments/grains are annotated on relevant drill holes. Only those drill holes that were analysed in the laboratory were tested for carbonate and had any magnetic response recorded. The extent of the high magnetic signature, as depicted on the 1.5VD (vertical derivative) processed aeromagnetic image, is also annotated on the sections. Facies interpretation between drill holes is limited to data available.

A ubiquitous 0.5-3 m thick surface regolith layer impregnated with silt coats the landsurface, whether on siltstone or sandstone saprolite, or on variable palaeosediments. The silt size material is most likely interpreted as aeolian dust (see section above), which has been mixed in with gravels, clays and sands of alluvial and colluvial sediments, or saprolite, to become parna. Silt size quartz grains may have been locally blown around from weathered siltstone bedrocks, but silt size clay aggregates may have been blown in from hundreds of kilometres to the west. Thus geochemical sampling within this layer is hazardous. The drill hole logs and interpreted regolith profiles give the specific material composition of this layer. The regolith landform units indicate the dominant geomorphic processes operating presently.

Broad areas of preserved palaeosediments up to 7 km wide and 40 m thick infill palaeovalleys, and in places overtop palaeovalley interfluves and bury palaeohighs. The palaeorelief is generally greater than present relief. The palaeosediments are eroded to various degrees and occur in all parts of the present landscape: beneath modern alluvium; partly inverted in relief covered by colluvial sheetwash; and fully inverted on crests. Thus the modern processes disguise the underlying palaeosediments. Sediment facies may vary from palaeovalley to top of buried interfluve, and between tributary palaeovalleys. The spacing of drill holes was not adequate in some areas to depict possible buried interfluves. Some grey clays contain floating rounded quartz grains and may be indicative of gelifluction, ie. gravity slumping of water saturated sediment. The distinctive grey clay profiles (eg. CBAC12, 16,18,90,92,96) may be an older generation of sediments than the mixed sand/gravel/clay profiles, but no suitable samples for palynological dating were found. Reconstruction of a minimum height of depositional surface prior to erosion indicates palaeosediment would have overtopped some local present drainage divides.

The *in situ* regolith is dominantly saprolite from highly weathered siltstone and, to a lesser extent, sandstone bedrock, with minor conglomerate at CBAC111. The lithology of some saprolite was not discerned. Vein quartz is common, and siliceous induration and chert is prevalent in places. Ferruginous induration, mottling and iron staining also occur. CBAC13 has much siliceous and ferruginous induration and vein quartz in both the bleached saprolite and siltstone saprolite. Bleached saprolite zones are commonly associated with the base of palaeovalleys infilled with palaeosediments, eg. CBAC12, 14, 18, 35, 48, 52, etc. which were, and in some cases still are, areas of saturation and deep weathering with leaching of soluble elements. CBAC 52 has a bleached zone extending at least 30m below the base of the palaeovalley sediments. The bleached zone at CBAC124 may relate to palaeosediments that have been entirely eroded out. Some bleached zones are unrelated to palaeovalley sediments, eg. CBAC65, 70, 88, 114, 133, etc. and may relate to structurally defined pathways for preferential fluid flow, of lithologically less resistant rocks, eg. CBAC114 (cf. magnetic low).

3.9 Regolith and Landform Evolution

The lack of dating of the palaeosediments makes the history of landform and regolith evolution somewhat indeterminate. However, a likely sequence of events can be established. A former Mesozoic cover extending from the Eromanga Basin to the north and Surat Basin to the northeast is inferred over this area. The only dated remnant of this cover occurs 60 km west of Cobar (Gibson, 1999). White clay indurated quartz/lithic conglomerate, sandstone and shale sediments at Coolabah immediately east of the study area on the Macquarie/Bogan-Darling drainage divide are very similar in the field to dated Jurassic sediments near Parkes and Molong on the Lachlan-Macquarie divide (Gibson and Chan, 1999). Apatite fission track data from around Cobar defines an Early Tertiary cooling event (O'Sullivan et al, 1998) which could be interpreted as the denudation of this Mesozoic cover due to the initiation of the Murray Basin and its associated low base level.

Over much of the northern Lachlan Fold Belt incision in the Early Tertiary exhumed north trending pre cover structural palaeovalleys (Chan, 1999; Gibson and Chan, 2000). Some of these palaeovalleys run along faults, eg. the Rookery Fault north of Cobar (Ford, 1996). It is possible that the Mulga Creek palaeovalley system in the centre of the study area is one such exhumed palaeovalley, which may contain some remnant basal Mesozoic sediments. Continued incision penetrated the Mesozoic unconformity into the underlying basement rocks of the Lachlan Fold Belt and progressed upstream into tributaries via headward erosion.

Alluviation of this dissected topography commenced in the Early Tertiary in incised palaeovalleys adjacent to and entering the Murray Basin from the Lachlan Fold Belt. Leucitite flows around 'El Capitan' within the study area issued from local plugs to the south along a north trending fracture line and inflated (O. Gonzalez, Honours Thesis, CRC LEME, U.C.) in the Miocene at 14.87Ma (Phillips, 2001.). O. Gonzalez's studies show that the lavas infill shallow valleys and overlie a Mid Miocene (B. Pillans, pers. comm., 2001) ferruginous weathering profile. The change from a warm wet climate with high water table and iron in solution to a warm dry climate with lower water table in the mid Miocene caused oxidation of the iron impregnated regolith, especially along drainage lines. Local evidence of this widespread mid Miocene ferruginisation event is at 'El Capitan', Wilga Tank, Elura and McKinnons Mines (B. Pillans, pers. comm., 2001). Relief inversion occurred as the indurated regolith is more resistant to weathering and erosion than surrounding non-indurated regolith.

Some of the Early Tertiary sediments may have been eroded in the Late Miocene (6-11Ma) due to a global sea level fall, and may relate to the Mologa Surface. Alluviation recommenced throughout the north Lachlan Fold Belt from the end of the Miocene, probably due to rising base levels in the Murray Basin and the change to a drier climate. It continued during the late Tertiary and the Quaternary, incorporating the eroded ferruginous saprolite mottles and ferricrete fragments, which were converted to maghemite during transport. Each layer of magnetic sediments in the drill hole profiles probably represents the first depositional event in a new erosion cycle. A major time transgressive hiatus in sedimentation from the Late Pliocene to Pleistocene, and ensuing erosion, is evident in some areas, eg. the hiatus between the Lachlan Formation (reduced environment) and the Cowra Formation (oxidising environment) in the Lachlan River system (Williamson, 1986). Perhaps the grey clays in the study area are equivalent in age and depositional environment to the Lachlan Formation. Gelifluction of some grey clays containing rounded sand grains may have occurred due to water soaked ground in a wetter phase during this period.

Sediments include both alluvium from through flow and colluvium from valley sides. Logging of drill hole materials indicates sedimentation overtopped the palaeovalley interfluves in at least some locations (CBAC33, 34, 49, 50, 102, 104). Erosion of the upper palaeovalley sediments is also apparent, with some sediments inverted in relief. The palaeodivides of the palaeovalleys with presently preserved magnetic palaeosediments are likely to be similar to the Early Tertiary palaeodivides prior to alluviation of the palaeovalleys. The palaeodivides may have shifted in the intervening period if continued sedimentation overtopped the palaeodivides prior to eroding back to the present distribution of palaeosediments. Erosion and sedimentation continues in balance today, with independent thresholds in different local catchments.

The products of present land surface processes mask much of the underlying saprolite and palaeosediments in the study area. Colluvial sheetwash predominates, with alluvial sediments in modern drainage tracts. Residual soils and lag occur on some crests. Aeolian dust acquisition appears to be ubiquitous across the study area on all landscape elements, and reflects increased aridity in the recent geological past. A silt size component (including clay aggregates) occurs in almost all soils whether on siltstone or sandstone saprolite, or clay/sand/gravel palaeosediments. Also, soils on quartz free leucitite soils on top of mesas at 'El Capitan' have 50% quartz, which has been added by aeolian accession (pers. comm. O.Gonzalez, 2001). Pedogenesis has mixed this aeolian dust into the surface sediment and residual soils to give a 0.5 to 3 m thick layer of parna.

4 REFERENCES

ALIPOUR, S., COHEN, D.R. and DUNLOP, A.C., 1997. Characteristics of magnetic and non-magnetic lag in the Cobar area, NSW. Journal of Geochemical Exploration. 58: 15-28

BUREAU OF METEOROLOGY, 2001. Web site.

BUTLER, B. E., 1956. Parna - an aeolian clay. Australian Journal of Science. 18: 145-151.

CAIRNS, C.J., McQUEEN, K.G. and LEAH, P.A., 2001. Mineralogical controls on element dispersion in regolith over two mineralised shear zones near the Peak, Cobar, New South Wales. Journal of Geochemical Exploration. 72: 1-21.

CHAN, R. A., 1999. Palaeodrainage and its significance to mineral exploration in the Bathurst region, NSW. Proceedings from Regolith 1998 Conference, Kalgoorlie, May 1998. CRC LEME, Perth. 38-54.

DICKSON B.L. and SCOTT, K.M., 1998. Recognition of aeolian soils of the Blayney district, NSW: Implications for exploration. Journal of Geochemical Exploration: 63, 237-251.

EGGLETON, R.A., 2001 The Regolith Glossary, surficial geology, soils and landscapes. CRC LEME. 152pp.

FLEMING, G. and HICKS, M., 2000. Preparations for shallow reconnaissance drilling, Sussex area. Cobar, NSW. NSW Department of Mineral Resources Report GS 2000/579. 11pp.

FLEMING, G., HICKS, M and Barron, L., 2001. First programme of shallow reconnaissance aircore drilling, Sussex area. Cobar, NSW. NSW Department of Mineral Resources Report GS 2001/200.

FOGARTY, M. and HASTINGS, R., 2001. Tritton copper deposit project update. Minfo, 69: 34-36.

FORD, A.J., 1996. Re-interpreting the north eastern margin of the Cobar Basin using drainage channel morphology. In Cook, W.G., Ford, A.J.H., McDermott, J.J., Standish, P.N., Stegman, C.L. and Stegman, T.M. (Eds.), The Cobar Mineral Field – a 1996 perspective. Australasian Institute of Mining and Metallurgy, Melbourne. Spectrum Series. 113-123.

FORSTER, D.B. and SECCOMBE, P.K., 2000. Syntectonic base metal and epithermal gold mineralisation: the McKinnons gold deposit, Cobar, NSW, Australia. In McQueen, K.G. and Stegman, C.L, (Eds.), Central West Symposium, Cobar 2000: Extended Abstracts. CRC LEME, Perth. 25-30.

GIBSON, D.L., 1999. Explanatory notes for the 1:5000 000 Cobar Regolith Landform map. CRC LEME Open File Report 76. 53pp.

GIBSON, D.L. and CHAN, R.A., 1999. Aspects of palaeodrainage of the north Lachlan Fold Belt region. Proceedings from Regolith 1998 Conference, Kalgoorlie, May 1998. CRC LEME, Perth. 23-37.

GIBSON, D.L. and CHAN R.A., 2000. Regolith materials and landscape evolution. In Lyons P., Raymond O.L. and Duggan M.B. (Cmpls. and Eds.), Forbes Geological Sheet 1:250K SI55-7: Explanatory Notes, Chapter 19. AGSO Record 2000/20. 198-201.

GILLIGAN, L.B., 1974. Cobar and Mineral Hill synclinorial zones. In Markham, N.L. and Basden, H. (Eds.), The Mineral Deposits of New South Wales. Geological Survey of New South Wales, Sydney. 149-171.

GILLIGAN, L.B., 1982. The origin and evolution of the Mount Boppy Gold Deposit, Canbelego, and related mineralisation. M. App. Sci. thesis, New South Wales Institute of Technology, Sydney (unpublished). 198 pp.

GILLIGAN, L.B. and BYRNES, J.G., 1995. Cobar 1:250 000 Metallogenic Map, SH/55-14: metallogenic study and mineral deposit data sheets. Geological Survey of New South Wales, Sydney. 240pp.

GLEN, R.A. and FLEMING, G., 2000. A new exploration province in New South Wales: The "Girilambone Group". In McQueen, K.G. and Stegman, C.L, (Eds.), Central West Symposium, Cobar 2000: Extended Abstracts. CRC LEME, Perth. 36-37.

GLEN, R.A., 1987. Copper and gold rich deposits in deformed turbidites at Cobar, Australia: their structural control and hydrothermal origin. Economic Geology. 82: 124-140.

GONZALEZ, O.R., 2001. The geology and landscape history of the "El Capitan" area, Cobar, New South Wales. Unpublished Honours Thesis, University of Canberra.

GREENE, R.S.B., 1992. Soil physical properties of three geomorphic zones in a semi-arid mulga woodland. Australian Journal of Soil Research. 30: 55-69.

GREENE, R.S.B., GATEHOUSE, R., SCOTT, K.M., and CHEN, X.Y., 2001. Aeolian dust: implications for Australian mineral exploration and environmental management. Australian Journal of Soil Research. 39: 1-6.

GREENE, R.S.B., and NETTLETON, W.D., 1995. Soil genesis in a longitudinal dune - swale landscape, NSW, Australia. AGSO Journal of Australian Geology and Geophysics. 16: 277-287.

GREENE, R.S.B. and TONGWAY, D.J., 1989. The significance of (surface) physical and chemical properties in determining soil surface conditions of red earths in rangelands. Australian Journal of Soil Research. 27: 213-225.

HALLBERG, J.A., 1984. A geochemical aid to igneous rock-type identification in deeply weathered terrain. Journal of Geochemical Exploration. 20: 1-8.

HELLMAN, P.L., 1991. Girilambone copper project: resource study. Nord Resources (Pacific) Pty. Ltd., Internal Report (unpublished).

IDNURM, M. and SENIOR, B.R., 1978. Palaeomagnetic ages of weathered profiles in the Eromanga Basin, Queensland. Palaeogeography, Palaeoclimatology, Palaeoecology. 24: 263-277.

JESSUP, R.W., 1961. Evolution of the two younger (Quaternary) soil layers in the south-eastern portion of the Australian arid zone 1. The Parakylia layer, and 2. The Bookaloo layer. Journal of Soil Science. 12: 52-63 (part 2: 64-72).

LOVEDAY, J., 1974. Methods of analysis of irrigated soils. Bureau of Soils Technical Communication. 54.

MARSHALL, S.M. and SCOTT, K.M., 1999. Supergene derived McKinnons Gold Deposit and associated features in the surrounding weathered rock. In Taylor, G. and Pain, C. (Eds.), New approaches to an old contintent. Proceedings of Regolith 98. CRC LEME Perth. 149-154.

McGOWRAN, B., and LI, Q., 1998. Cainozoic climate change and its implications for understanding the Australian regolith. In Eggleton, R.A. (Ed.), The state of the regolith. Proceedings of the Second Australian Conference on Landscape Evolution and Mineral Exploration, Brisbane, Queensland, 1996. Geological Society of Australia, Special publication. 20: 86-103.

McQUEEN, K.G. and SPRY, M.J., 2000. Landscape-regolith controls on mineral exploration in the Cobar region of NSW. In McQueen, K.G. and Stegman, C.L, (Eds.), Central West Symposium, Cobar 2000: Extended Abstracts. CRC LEME, Perth. 65-67.

McQUEEN, K.G., HILL, S.M. and FOSTER, K.A., 2000. The gold-calcrete association in western NSW: How to find the next Cobar Goldfield. In McQueen, K.G. and Stegman, C.L, (Eds.) Central West Symposium, Cobar 2000: Extended Abstracts. CRC LEME, Perth. 60-64.

NORD PACIFIC LTD, 1998. Tritton copper deposit. Minfo. 61: 33-36.

O'SULLIVAN P.B., KOHN B.P. 1998, and MITCHELL M.M., 1998. Phanerozoic reactivation along a fundamental Proterozoic crustal fault, the Darling River lineament, Australia: constraints from apatite fission track thermochronology. Earth and Planetary Science Letters. 164: 451-465.

PAIN, C.F., CHAN, R.A., CRAIG, M.A., GIBSON, D.L., KILGOUR, P. and WILFORD, J.R., in press. RTMAP regolith database: field book hand users guide. Second edition. CRC LEME Report 138.

PATERSON, R.G., 1974. The geology and economic potential of the Nymagee mine. Cyprus Mines Corp. Unpublished report.

PHILLIPS, D., 2001. K-Ar analyses of leucitite sample WT6. Prise Report R2K-1070. Unpublished report. 3 pp

PONTUAL S., MERRY N., and GAMSON P., 1997. Spectral interpretation field manual. G – MEX Version 1.0. AusSpec International Pty.Ltd.

RENGASAMY, P., GREENE, R.S.B., FORD, G.W., and MEHANNI, A.H, 1984. Identification of dispersive behaviour and the management of red-brown earths. Aust. Journal of Soil Research. 22: 413-431.

RUGLESS, C.R., WILLIAMS, R.E. AND VANDERPLANK, A., 2000. Primary geochemical trends preserved in the regolith and implications for regional exploration for McKinnons-style gold mineralisation in the Cobar region. In McQueen, K.G. and Stegman, C.L, (Eds.), Central West Symposium, Cobar 2000: Extended Abstracts. CRC LEME, Perth. 78-86.

SCOTT, K.M., 1987. The mineralogical distribution of pathfinder elements in gossan derived from dolomitic shale-hosted Pb-Zn deposits, northwest Queensland, Australia. Chemical Geology. 64: 295-306.

SCOTT, K.M., 1997. The significance of Campaspe-dominated terrains in exploration within the Mt Windsor Sub-province, N.E. Queensland. CRC LEME Restricted Report 58R / CSIRO Exploration and Mining Report 422R. CRC LEME, Perth. 33pp.

SCOTT, K.M., 1999. Regolith effects and Au exploration in the Blayney-Orange district, NSW. In Taylor, G. and Pain C. (Eds.), New approaches to an old continent. Proceedings of Regolith 98. CRCLEME, Perth. 109-116.

SHIELDS, P., 1996. Geology of the Girilambone Copper Deposit. In Cook, W.G., Ford, A.J.H., McDermott, J.J., Standish, P.N., Stegman, C.L. and Stegman, T.M. (Eds.). The Cobar Mineral Field – a 1996 Perspective. Australasian Institute of Mining and Metallurgy, Melbourne. Spectrum Series. 3/96: 293-304.

SPRIGG, R.C., 1982 Alternating wind cycles of the Quaternary era, and their influence on aeolian sedimentation in and around the dune deserts of south eastern Australia. In Wasson, R.J. (Ed.), Quaternary dust mantles of China, New Zealand and Australia. Proceedings INQUA Loess Commission Workshop, Canberra, December, 1980.

SPRY, M.J., in prep. Regolith and landscape evolution of the Cobar area, NSW, Australia. University of Canberra PhD Thesis.

STEGMAN, C.L. AND POCOCK, J., 1996. The Cobar Gold Field – a geological perspective. In Cook, W.G., Ford, A.J.H., McDermott, J.J., Standish, P.N., Stegman, C.L. and Stegman, T.M. (Eds.), The Cobar Mineral Field – a 1996 Perspective. Australasian Institute of Mining and Metallurgy, Melbourne. Spectrum Series 3/96: 229-264.

STEGMAN, C.L. AND STEGMAN, T., 1996. The history of mining in the Cobar Field. In Cook, W.G., Ford, A.J.H., McDermott, J.J., Standish, P.N., Stegman, C.L. and Stegman, T.M. (Eds.), The Cobar Mineral Field – a 1996 perspective. Australasian Institute of Mining and Metallurgy, Melbourne. Spectrum Series 3/96: 3-39.

STEGMAN, C.L., 2000. The New Occidental Deposit: variation on a theme. In McQueen, K.G. and Stegman, C.L, (Eds.), Central West Symposium, Cobar 2000: Extended Abstracts. CRC LEME, Perth. 107-112.

SUPPEL, D.W. AND GILLIGAN, L.B., 1993. Nymagee 1:250 000 Metallogenic Map SI/55-2: metallogenic study and mineral deposit data sheets. 171 pp. Geological Survey of New South Wales, Sydney.

SUTHERLAND, F.L., 1985. Regional controls in eastern Australian volcanism. In Sutherland, F.L., Franklin, B.J. and Waltho, A.E. (Eds.), Volcanism in eastern Australia. Geological Society of Australia, NSW Division. 1: 13-32.

TAN, K.P., CHEN, X.Y. AND MCQUEEN, K.G., 1998. Aeolian component of soil profiles at the McKinnons Gold Deposit area, Cobar, New South Wales. Aeolian dust: implications for Australian mineral exploration and environmental management. CRC LEME Symposium, Australian National University, 25-26 November: Abstracts.

WALKER, P.J., 1991. Land systems of New South Wales. Soil Conservation Service for NSW Sydney.

WILLIAMSON W.H., 1986. Investigation of the groundwater resources of the Lachlan Valley alluvium. Part 1: Cowra to Jemalong Weir. Water Resources b Commission. Hydrological Report. 1986/12.

5 APPENDIX 1 - Laboratory Logging Sheet

Hole Id:	Location:	AMG Northing:		Elev (asl):	Logged by:	Sheet __ of __
Site Id:	Company:	AMG Easting:		EOH:	Date:	
Landform:		Dip:	Asimuth:	Datum:	Material type: chips / core	

graphic	depth	drilled material				colour				texture			common minerals														mag sus	transported qtz size							round			indurn/ concret				parent rock type		interp				additional info
	- to	aggregate	disaggregated	chip weak	chip strong	dominant	minor 1	minor 2	mottles	clay /silt %	sand %	gravel %	qtz	kao	other clay	magh	hem	goe	Mnox	carb	gypsum	mica	feld	ferromag	py	other		vein qtz	silt	vf-f	m	c-vc	granule	pebble	r	sr-sa	a	ferrug	calc	silic		nod/piso	relict primary text	Transported	Saprolite	Saprock	Bedrock	including alteration, unconformity, oxidation, palaeowatertable, palaeosol, channel sediments, etc

Drilled material:	**Colour:** Munsell charts s - soil (1992) r - rock (1963)	**Comments:**	Other data:
aggregate - appears to be formed by drilling process	**Parent rock type:** noted for in situ material		previous log
disaggregated - such as powder or loose gravels	**Saprolite**[1]**:** >20% minerals weathered, generally collapses under light blow		geochem
chip weak - easily broken between fingers	**Saprock**[1]**:** <20% minerals weathered, requires hammer blow to break		geophys
chip strong - not easily broken between fingers	[1]Eggleton (Ed) 1999 Glossary of regolith - draft		PIMA
			mag sus

6 APPENDIX 2 - Abundance of Carbonate in Selected Drill Holes

(M= Major fizz and m= minor fizz).

depth	cbac1	cbac4	cbac10	cbac12	cbac16	cbac18	cbac43	cbac48	cbac49	cbac51	cbac52	cbac53	cbac54	cbac63	cbac68	cbac72	cbac73	cbac74
0	m	m	m	m	m	m	m	m	m	m	m	m	m	m	m	m		
1	m	m	m	m	M	m	m	m	m	m	m	m	m		m	m		
2	m	M	M	m	M	m	m	m	m	m	M				M	m		
3	m	M	m	m	M	M	m	M	m	M	M				M	m	m	m
4				M	M		M		m		M				m	m		
5				m	M				M							m		M
6				m	M											M		
7				m	m							m					m	M
8				m	M													
9				M														m
10				m							m							
11											m							
12											M		m					
14													m					
16																		
18																	M	
20																		
22																		
24																		
26																		
28																		
30																		
32																		
34																		
36																		

cbac75	cbac76	cbac77	cbac78	cbac81	cbac83	cbac90	cbac92	cbac95	cbac97	cbac99	cbac100	cbac102	cbac103	cbac104	cbac105	cbac106	cbac111
	m	m	m		m	m	m	m	m		m		m	m	m	m	
	m	m	m		m		m		M								
		M		m	M		M		M	m	m	M		M	M	m	
m					m		M		M	m		M		M	M	M	
M			m						M						m	M	m
M			m						M							m	
M								M								m	
M								M									
M																	
																m	
																M	
	M	m															

cbac120	cbac121	cbac122	cbac129	cbac137	cbac138
m					
m	m				
m	M	m			
m	M			M	
m	m				
	m				M
	m				
	m				
			m		m

7 APPENDIX 3 - Depth of the Unconformity

(Transported/*in situ* boundary)

FIELD ID	SITE ID	Base T(m)
CBAC001	200170001	3
CBAC004	200170004	1
CBAC010	200170010	1
CBAC012	200170012	20
CBAC016	200170016	6
CBAC018	200170018	16
CBAC043	200170043	1
CBAC048	200170048	16
CBAC049	200170049	6
CBAC051	200170051	14
CBAC052	200170052	13
CBAC054	200170054	20
CBAC063	200170063	2
CBAC068	200170068	2
CBAC072	200170072	16
CBAC073	200170073	20
CBAC074	200170074	30
CBAC075	200170075	32
CBAC076	200170076	30
CBAC077	200170077	32
CBAC078	200170078	24
CBAC080	200170080	10
CBAC081	200170081	2

CBAC083	200170083	2
CBAC090	200170090	16
CBAC092	200170092	26
CBAC095	200170095	11
CBAC097	200170097	1
CBAC099	200170099	22
CBAC100	200170100	5
CBAC102	200170102	5
CBAC103	200170103	22
CBAC104	200170104	5
CBAC105	200170105	16
CBAC106	200170106	12
CBAC111	200170111	1
CBAC120	200170120	1
CBAC121	200170121	2
CBAC122	200170122	1
CBAC129	200170129	7
CBAC137	200170137	12
CBAC138	200170138	22

8 APPENDIX 4 – Definitions

saprock Compact, slightly weathered rock with low porosity; defined as having less than 20% of weatherable minerals altered but generally requiring a hammer blow to break. Weathering effects are present mainly at the micro-sites of contacts between minerals and intra-mineral fissures, along shears and fractures through the rock as a whole, or affecting only a few individual mineral grains or mineral species. The first signs of weathering are generally oxidation of sulphides and iron-bearing silicates or breakdown of feldspars to clays. The gradational boundaries of the saprock may be difficult to locate at the hand specimen scale as it is difficult to determine the proportion of weatherable minerals in the fresh rock without a detailed petrographic study.

saprolite From Greek rock, σαπρος (sapros) and λιθος (lithos), putrid. Weathered bedrock in which the fabric of the parent rock, originally expressed by the arrangement of the primary mineral constituents of the rock (e.g. crystal, grains), is retained. Compared to saprock, saprolite has more than 20% of weatherable minerals altered, and generally collapses under a light blow. Saprolite may be extended to include weathered rocks in which only larger structures such as bedding, schistosity, veining or lithological contacts are preserved. The presence of saprolite implies that weathering has been essentially isovolumetric. Saprolite is commonly the material referred to as the C horizon in pedology.

saprolith The saprolith is the (generally lower) part of the regolith that has retained the fabric of the parent rock. That is, saprock plus saprolite. The definition may include weathered rocks in which only larger structures including bedding, schistosity, veining or lithological contacts are preserved. The presence of these fabric elements implies that weathering has been essentially isovolumetric, pseudomorphic and *in-situ*.

9 APPENDIX 5 – List of data available from this study

Data available as a joint NSWDMR / CRC LEME release on the NSWDMR website via *DIGS (www.minerals.nsw.gov.au) and on CD ROM****

.

GS2001/319 (CRC LEME)

1 PIMA traces and logs of 42 selected drill holes;
2 Microscopy logs of 33 drill holes down loaded from AGSO's Deviant database (xls)
3 Regolith Landform Map (Preliminary);
4 Regolith profile sections for the 3 traverses.

GS2001/200 (NSWDMR)

1. Field logs for all 138 drill holes (logged by B. Maly, CRC LEME);
2. Complete geochemical analyses for 22 elements
3. Images of chip trays samples from all 138 drill holes (imaged by B. Maly, CRC LEME);
4. Preliminary petrological analyses of 138 thin sections

A CD ROM containing the above reports and data from GS2001/200 and GS 2001/319 in document-quality pdf format and MS-Excel format is also available**.

- ***DIGS*** is the NSW Department of Mineral Resources digital image-based report viewing system which is accessible via the internet.

****Contact Mick May (NSWDMR) to order a CD ($20.00 incl. GST) – phone 02 9901 8491